Distributions of Time to First Spot Fire

by

Trevor James Thomson

B.Sc., University of Winnipeg, 2015

Thesis Submitted in Partial Fulfillment of the
Requirements for the Degree of
Master of Science

in the
Department of Statistics and Actuarial Science
Faculty of Science

SIMON FRASER UNIVERSITY
Summer 2017

Approval

Name:	**Trevor James Thomson**
Degree:	**Master of Science (Statistics)**
Title:	***Distributions of Time to First Spot Fire***
Examining Committee:	**Chair:** Tim Swartz Professor

X. Joan Hu
Senior Supervisor
Professor
Department of Statistics and Actuarial Science
Simon Fraser University

W. John Braun
Supervisor
Professor
Department of Computer Science, Mathematics, Physics, and Statistics
The University of British Columbia - Okanagan

David Alexander Campbell
Internal Examiner
Associate Professor
Department of Statistics and Actuarial Science
Simon Fraser University

Date Defended: August 15, 2017

Abstract

In wildfire management, a spot fire is the result of an airborne ember igniting a separate fire away from the main wildfire. Under certain environmental and wildfire conditions, a burning ember can breach a fuel break, such as a river or road, and result in the production of a spot fire. This project derives distributions of the time to the first spot fire in various situations, and verifies them by simulation. To demonstrate the implementation of the distributions in practice, we incorporate a stochastic fire spread model. This research assesses the likelihood of spot fire occurring passed a fuel break, all while taking into account both spotting distance and spotting rate. This contrasts with the traditional approach that solely involves the maximal spotting distance, and can be a tool for fire management.

Keywords: Firebrand; Mixture distribution; Poisson process; Simulation; Wildfire modelling

Acknowledgements

First of all, I would like to express my sincere gratitude to my co-supervisors, John Braun and Joan Hu. Thank-you John for the opportunity to work on a very stimulating problem, and your support throughout the past two years. Thank-you Joan, not only for your patience and encouragement, but your instruction, care, and preparing me to in becoming a well-rounded statistician. I feel truly blessed to have been your student!

To my fellow graduate students, specifically JinChoel Choi, Mike Grosskopf, Tianyu Guan, Khalif Halani, Grace Hsu, Dongdong Li, Tian Li, Lillian Lin, Moyan Mei, Jacob Mortensen, Jennifer Parkhouse, Will Ruth, Abdollah Safari, Nate Sandholtz, Perry Sang, Chenlu Shi, Terry Tang, Michelle Thiessen, Matthew van Bommel, Steven Wu, Yi Xiong, Yuping Yang, Joanna Zhao, Charlie Zhou, and Zhiyang Zhou. Thank-you for the many stimulating discussions, words of encouragement, and laughs we shared together.

I would like to thank my course instructors - Rachel Altman, Luke Bornn, Dave Campbell, Joan Hu, Boxin Tang, and Steve Thompson - for their valuable lessons through their outstanding lectures. I have learned a lot over the past two years, and you have shown me why SFU is one of the top universities in Canada.

To my girlfriend, Jiying, thank-you for your support, patience, and comfort during challenging times. Your positivity has always brightened my spirits, and I could not have achieved my goals without you!

Last, but certainly not least, I would like to thank my parents and brothers - Jonathon and Shawn - for their endless love and support. Although they are halfway across the country, their love and support have always been by my side!

Contents

List of Tables

List of Figures

Chapter 1

Introduction

1.1 Background

Wildfires are both natural and human caused phenomena that, on occasion, devastate communities and economies around the world. A notable example is the 2016 Fort McMurray, Alberta wildfire where the city was placed under mandatory evacuation, and resulted in approximately $3.58 billion worth of damage (Snowdon 2016). Several factors led to the event at Fort McMurray, one of which was the wildfire producing spot fires. A spot fire is the occurrence of airborne burning embers, referred to as firebrands, that ignites a new fire ahead of the main wildfire (Thomas and McAlpine 2010). Many spot fires occur near the main fire front and are of minimal interest, since the main wildfire engulfs the new fire before it significantly contributes to the rate of spread (Perryman *et al.* 2013). However, if a convection column is developed, spot fires can potentially occur several kilometres ahead of the main fire (Thomas and McAlpine 2010). Of special interest is the occurrence of a new fire spawning on the opposite end of a fuel break, such as a river or roadway. The significance of this event allows the wildfire to overcome natural barriers, and to possibly advance towards communities. For example, it was confirmed that spot fires occurred on the opposite side of both the Athabasca and Hangingstone rivers, which contributed to the wildfire reaching Fort McMurray (Ha 2016).

Due to the dangers that spot fires present, comprehending the fire spotting process has been an active research area within wildfire management. The common strategy within the literature is to decompose the entire spotting process into several sub-processes, and model each sub-process separately. Examples of these sub-processes include the potential of a firebrand to be sent aloft, the release of the firebrand from the convection column, the firebrand landing on combustible fuel, and the capability of a firebrand to remain burning throughout the entire operation. Albini (1979) was one of the first investigators to implement this strategy. Physical models pertaining to characteristics of wildfires were used to develop a

predictive model, although in an improvised manner, for the maximum distance a firebrand can travel. However, the model requires observations that are difficult to measure, such as the mass of a firebrand, the vertical wind speed profile, and the surface topography in the direction the firebrand is travelling (Finney 2004). Recent modelling of spot fires have been directed towards estimating the distribution of the distance firebrands travel. For example, Martin and Hillen (2016) obtained what they termed as a "spotting distribution", as the probability distribution of observing a spot fire at a particular location through a transport equation. Another model proposed by Boychuk *et al.* (2008) introduced a stochastic cellular automaton fire spread model, along with a fire spotting procedure. This method essentially simulated the distance firebrands travel along the convection column, and the landing location of descending firebrands. Although it was the first fire spread model to incorporate long-distance fire spotting, there are other complications within their spotting submodel, such as reliance on normality for the firebrand travelling distribution (Martin and Hillen 2016).

1.2 Objective and Outline

Although the cited works are important bridges to comprehend the fire spotting process, the likelihood of a spot fire occurring remains an open problem. Rather than centring our attention towards the distance firebrands travel, we focus on the rate at which firebrands are emitted from the wildfire. This will allow us to quantitatively assess the probability of a spot fire occurring within a specific location, such as passed a fuel break. This can ultimately assist with fire management resource allocation, and administration affairs when livelihoods are at risk.

We organize this project as follows. In Chapter 2, we undertake a counting process framework to derive the distribution of the time to the first spot fire. By imposing assumptions on the intensity function and probability of a firebrand resulting in a spot fire that travels the necessary distance, we can obtain a form pertaining to the distribution of the time to the first spot fire. Chapter 3 presents a simulation study where we numerically generate realizations of the time to the first spot fire, and offer a link between firebrand generation and wildfire modelling. A summary and an outlook for future research concludes this project in Chapter 4.

Chapter 2

Deriving Distributions of Time to the First Spot Fire

In this Chapter, we derive the distribution of the time to the first spot fire that crossed a fuel break. In other words, if we let W denote the time when a firebrand successfully ignites a new fire passed a fuel break, we proceed to derive $P(W \leq t)$ for any $t > 0$. The outline of this Chapter is as follows. Chapter 2.1 introduces the common notation used throughout this project, and is accompanied with preliminary definitions. We derive the marginal distribution of W in Chapter 2.2 after supplying the firebrand rate function over time, and the success probability for an individual firebrand to result in a spot fire. We then conclude this Chapter with an illustration with three examples in Chapter 2.3.

2.1 Preliminaries & Notation

Suppose that a wildfire is ignited at time $t = 0$ within a cell $s \in \mathscr{S}$, where $\mathscr{S}$ is a regular two-dimensional lattice. Let $N(t; s)$ denote the cumulative number of firebrands generated by the wildfire within cell s over the time interval $[0, t]$, where $t > 0$. With s fixed, we regard $\{N(t; s) : t > 0\}$ as a counting process with $\lambda(t; s)$ denoting the intensity function. Moreover, let $p(t; s)$ denote the probability that a firebrand generated within cell s at time t results in a spot fire that crossed a fuel break. Then given the time interval $[0, T^*]$, where $T^* > 0$ is the time point when we stop observing the wildfire, we utilize the theory behind counting processes to derive the distribution of the time to the first spot fire that crossed a fuel break.

For each $s \in \mathscr{S}$, let W_s denote the time to the first spot fire that crossed a fuel break caused by a firebrand generated within cell s. We then either have (i) $W_s \in [0, T^*]$, which means that we observed at least one firebrand generated within cell s that resulted in a spot fire that crossed a fuel break, or (ii) W_s is right-censored at time T^*, meaning that we were unable to observe a firebrand generated within cell s result in a spot fire that crossed a fuel

break over the interval $[0, T^*]$. To accommodate for this latter scenario, we assign $W_s = \infty$ if no spot fires occurred, so that $W_s \in [0, T^*] \cup \{\infty\}$, for every $s \in \mathscr{S}$. This allows us to investigate the time to the first spot that crossed a fuel break, which is $W = \min_{s \in \mathscr{S}}\{W_s\}$. In the case where $W_s = \infty$ for every $s \in \mathscr{S}$, we then have $W = \infty$, so that no spot fires crossed a fuel break over $[0, T^*]$.

In order for a spot fire to occur, Thomas and McAlpine (2010) outline three basic elements that must take place:

(i) A firebrand must be able to kindle a fire upon landing. If a firebrand is too moist, it is incapable of igniting a new fire. Conversely, if a firebrand is not moist enough, then the firebrand will burn-out prior to landing.

(ii) Fire whirls and the convection column must have sufficient convective energy to carry firebrands aloft.

(iii) The ground where a firebrand lands must be receptive to rapid ignition.

In addition to these three conditions, we require a fourth element if a firebrand is to cross a fuel break:

(iv) The firebrand must travel a sufficient distance in order to overcome the fuel break.

Overall, a variety of events must transpire in order for a spot fire to cross a fuel break, which may not be satisfied over the entire interval $[0, T^*]$. For example, the distance between the wildfire and a fuel break may be greater than the maximal spotting distance (Albini 1979). This means that none of the firebrands generated by the wildfire can possibly breach a fuel break, in which case, we have $p(t; s) = 0$. This motivates us to specify the probability of a firebrand generated within cell s at time resulting in a spot fire that crossed a fuel break as

$$p(t; s) = p_s I(t \in [t^p_{1s}, t^p_{2s}]), \tag{2.1}$$

where $p_s \in [0, 1]$ is, in general, an unknown parameter, and $[t^p_{1s}, t^p_{2s}] \subseteq [0, T^*]$, is a known time interval. With the counting process $\{N(t; s) : t > 0\}$ along with the probability $p(t; s)$, we proceed to derive

$$F_W(t) = P(W \leq t), \tag{2.2}$$

that is, the marginal distribution of W. Equivalently, we will derive

$$P(W > t) = 1 - F_W(t), \tag{2.3}$$

which is the survival function of W. Under the assumption that the times $\{W_s : s \in \mathscr{S}\}$ are mutually independent, we expand Equation (2.3) as

$$\begin{aligned} P(W > t) &= P\left(\min_{s\in\mathscr{S}}\{W_s\} > t\right) \\ &= P(W_s > t, \text{for all } s \in \mathscr{S}) \\ &= \prod_{s\in\mathscr{S}} P(W_s > t), \end{aligned} \tag{2.4}$$

and by the law of total probability, each term within Equation (2.4) becomes

$$P(W_s > t) = \begin{cases} 1 & \text{if } t < t^p_{1s} \\ \sum_{k=0}^{\infty} P(W_s > t | N(t;s) = k) P(N(t;s) = k) & \text{if } t^p_{1s} \le t \le t^p_{2s} \\ \sum_{k=0}^{\infty} P(W_s > t^p_{2s} | N(t^p_{2s};s) = k) P(N(t^p_{2s};s) = k) & \text{if } t^p_{2s} < t \le T^*. \end{cases} \tag{2.5}$$

We can see from Equation (2.4) that the survival function of W is obtained by calculating the joint survival function of $\{W_s : s \in \mathscr{S}\}$, which is the product of each W_s's marginal survival functions under the mutual independence assumption. In fact, we can see that W_s follows a mixture distribution, with components (i) the resulting distribution emerging from Equation (2.5), and (ii) a point mass distribution at $t = \infty$. The mixture weights are known however, since the weight of the point mass distribution is the accumulated mass that surpassed the censoring time T^*, which is $P(W_s > T^*)$.

2.2 Marginal Distribution of Time to the First Spot Fire

For each $s \in \mathscr{S}$, suppose that $\{N(t;s) : t > 0\}$ follows a Poisson process, which is a collection of point events that occur completely at random over the interval $[0, t]$ (Cox and Isham 1980). We further assume that the intensity function $\lambda(t;s) = \lambda_s(t)$ is a known function of t, but can vary over s. By specifying a form for $\lambda_s(t)$, this will aid us towards evaluating the survival function of W_s presented in Equation (2.5). First, let us consider the case where firebrands are generated at a constant rate over time.

2.2.1 Modelling Firebrand Generation Over Time as a Homogeneous Poisson Process

Suppose that a wildfire is able to generate firebrands within cell s over the interval $[0, \infty)$, and the intensity function is a homogeneous function of time. That is, the intensity function is $\lambda_s(t) = \lambda_s$, where λ_s is an unknown constant that may vary over cells $s \in \mathscr{S}$. Under this situation, $\{N(t;s) : t > 0\}$ is a homogeneous Poisson process, which is presented below.

Definition 2.2.1. Cox and Isham, (1980): Let $N(t;s)$ denote the number of firebrands generated by a wildfire in a fixed cell $s \in \mathscr{S}$ and time interval $[0,t]$. Then $\{N(t;s) : t > 0\}$ is a homogeneous Poisson process with intensity function $\lambda(t;s) = \lambda_s$ if

(i) $N(t;s) \sim \text{Poisson}(\lambda_s t)$,

(ii) $N(t;s)$ is independent of $N(t;s) - N(u;s)$ for any $0 < u \leq t$.

Note that because λ_s completely specifies the distribution of $N(t;s)$, we only need to specify λ_s, in order to evaluate $P(N(t;s) = k)$ in Equation (2.5). Moreover, since $N(t;s)$ follows a homogeneous Poisson process, the conditional distribution of the $N(t;s) = k$ firebrand arrival times is

$$(T_{1s}, \cdots T_{ks} | N(t;s) = k) \stackrel{d}{=} (U_{(1)}, \cdots, U_{(k)}),$$

where "$\stackrel{d}{=}$" is denoted as equal in distribution, T_{js} is the time when the j^{th} firebrand is generated within cell s, and $U_{(j)}$ is the j^{th} order statistic of k independent and identically distributed Uniform$(0,t)$ random variables. This allows us to calculate the probability of a firebrand generated within $[t^p_{1s}, t^p_{2s}]$, to be $P(U_j \in [t^p_{1s}, t^p_{2s}]) = \mathscr{L}([0,t] \cap [t^p_{1s}, t^p_{2s}])/t$, where $\mathscr{L}(\mathscr{A}) = |\mathscr{A}|$ is the length of the interval $\mathscr{A}$. In the case where $t \in [t^p_{1s}, t^p_{2s}]$, we see that $P(U_j \in [t^p_{1s}, t^p_{2s}]) = (t - t^p_{1s})/t$, which informs us that the arrival time of the j^{th} firebrand is uniformly distributed over $[0,t]$. Since we are primarily interested in firebrands that are generated within $[t^p_{1s}, t^p_{2s}]$, let $N^*(t;s) = N(t;s) - N(t^p_{1s};s)$. We can then condition on $N^*(t;s)$, and simplify Equation (2.5) for $t \in [t^p_{1s}, t^p_{2s}]$ as

$$\begin{aligned} P(W_s > t | N(t;s) = k) &= \sum_{\ell=0}^{k} P(W_s > t | N(t;s) = k, N^*(t;s) = \ell) P(N^*(t;s) = \ell | N(t;s) = k) \\ &= \sum_{\ell=0}^{k} (1-p_s)^\ell \binom{k}{\ell} \left(\frac{t - t^p_{1s}}{t}\right)^\ell \left(1 - \frac{t - t^p_{1s}}{t}\right)^{k-\ell} \qquad (2.6) \\ &= \sum_{\ell=0}^{k} \binom{k}{\ell} \left((1-p_s)\frac{t - t^p_{1s}}{t}\right)^\ell \left(1 - \frac{t - t^p_{1s}}{t}\right)^{k-\ell}. \qquad (2.7) \end{aligned}$$

Equation (2.6) follows from $P(W_s > t | N(t;s) = k, N^*(t;s) = \ell)$ being the probability that all ℓ firebrands generated within $[t^p_{1s}, t]$ fail to result in a spot fire, and by making use of the firebrand mutual independence assumption, this occurs with probability $(1-p_s)^\ell$. Also, $P(N^*(t;s) = \ell | N(t;s) = k)$ is the probability that ℓ of the k generated firebrands are developed in the time interval $[t^p_{1s}, t]$, which is Binomial$(k, (t - t^p_{1s})/t)$ distributed. By

letting $\pi_s = (t - t^p_{1s})/t$, Equation (2.7) becomes

$$\begin{aligned} P(W_s > t | N(t;s) = k) &= \sum_{\ell=0}^{k} \binom{k}{\ell} \left((1-p_s) \frac{\pi_s}{1-\pi_s} \right)^{\ell} (1-\pi_s)^k \\ &= \left(1 + (1-p_s) \frac{\pi_s}{1-\pi_s} \right)^{k} (1-\pi_s)^k \\ &= \left(1 - p_s \frac{t - t^p_{1s}}{t} \right)^{k} \\ &= q_s^k, \end{aligned} \tag{2.8}$$

where $q_s = 1 - p_s(t - t^p_{1s})/t$. By using Equation (2.8) and Definition 2.2.1, Equation (2.5) simplifies to

$$\begin{aligned} P(W_s > t) &= \sum_{k=0}^{\infty} q_s^k \frac{(\lambda_s t)^k}{k!} \exp(-\lambda_s t) \\ &= \exp(-\lambda_s t) \underbrace{\sum_{k=0}^{\infty} \frac{(\lambda_s q_s t)^k}{k!}}_{\exp(\lambda_s q_s t)} \\ &= \exp(-\lambda_s t(1 - q_s)) \\ &= \exp\left(-\lambda_s p_s (t - t^p_{1s})\right). \end{aligned}$$

Overall, Equation (2.5) is simplified for any t as

$$P(W_s > t) = \begin{cases} 1 & \text{if } t < t^p_{1s} \\ \exp\left(-\lambda_s p_s (t - t^p_{1s})\right) & \text{if } t^p_{1s} \le t \le t^p_{2s} \\ \exp\left(-\lambda_s p_s (t^p_{2s} - t^p_{1s})\right) & \text{if } t^p_{2s} < t \le T^*, \end{cases} \tag{2.9}$$

and $P(W_s = \infty) = P(W_s > T^*)$ is the mass at time $t = \infty$. Equation (2.9) reveals to us that for any $s \in \mathscr{S}$, W_s follows a mixture distribution composed of (i) a shifted Exponential distribution with shift parameter t^p_{1s} and rate parameter $\lambda_s p_s$ with support $t \in [t^p_{1s}, t^p_{2s}]$, and (ii) a point mass distribution at $t = \infty$. With the survival function of W_s derived, we can insert Equation (2.9) into Equation (2.4), and obtain the survival function of W as

$$P(W > t) = \begin{cases} 1 & \text{if } t < t^p_1 \\ \exp\left(- \left\{ \sum_{s \in \mathscr{S}} \lambda_s p_s \left[t I(t \in [t^p_{1s}, t^p_{2s}]) + t^p_{2s} I(t > t^p_{2s}) - t^p_{1s} I(t \ge t^p_{1s}) \right] \right\} \right) & \text{if } t^p_1 \le t \le T^*, \end{cases} \tag{2.10}$$

and $P(W = \infty) = \prod_{s \in \mathscr{S}} P(W_s > T^*)$ is the probability of zero spot fires occurring passed a fuel break over the time interval $[0, T^*]$, where $t_1^p = \min_{s \in \mathscr{S}}\{t_{1s}^p\}$.

2.2.2 Modelling Firebrand Generation Over Time as a Non-homogeneous Poisson Process

Although a variety of phenomena can be adequately modelled with the homogeneous Poisson process in Chapter 2.2.1, the assumption of a constant intensity function is unrealistic within our setting. As shown in Figure A.1, it is likely that there exists a cell $s \in \mathscr{S}$ that is incapable of generating firebrands at time $t = 0$, or the intensity function of $\{N(t; s) : t > 0\}$ may not be a constant function with respect to time. That is, each $s \in \mathscr{S}$ can generate firebrands within a certain time interval $[t_{1s}^\lambda, t_{2s}^\lambda] \subseteq [0, T^*]$, and $\lambda(t; s) = \lambda_s(t)$ is not necessarily a temporal homogeneous function. A more realistic scenario is to associate $[t_{1s}^\lambda, t_{2s}^\lambda]$ with the time interval when cell s is burning. All that we require however, is $[t_{1s}^p, t_{2s}^p] \subseteq [t_{1s}^\lambda, t_{2s}^\lambda]$, so that there is a time interval for firebrands generated within cell s to potentially result in a spot fire that crossed a fuel break. This motivates us to utilize the non-homogeneous Poisson process, which is presented below.

Definition 2.2.2. Cox and Isham, (1980): Let $N(t; s)$ denote the number of firebrands generated by a wildfire at a fixed cell $s \in \mathscr{S}$ and time interval $[0, t]$. Then $\{N(t; s) : t > 0\}$ is a non-homogeneous Poisson process with intensity function $\lambda(t; s) = \lambda_s(t)$ if

(i) $N(t; s) \sim \text{Poisson}(\Lambda_s(t))$, where

$$\Lambda_s(t) = \mathrm{E}\{N(t; s)\} = \int_0^t \lambda_s(u)du$$

(ii) $N(t; s)$ is independent of $N(t; s) - N(u; s)$ for any $0 < u \leq t$.

As discussed in Chapter 2.2.1, $\lambda_s(t)$ completely specifies the distribution of $N(t; s)$, so that $P(N(t; s) = k)$ in Equation (2.5) can be evaluated once we specify $\lambda_s(t)$. However, since the non-homogeneous Poisson process is not a stationary process, this prevents us from directly using the results pertaining to the homogeneous Poisson process. After performing a deterministic time change, the non-homogeneous Poisson process reduces to a homogeneous Poisson process with intensity $\lambda_s = 1$. To see why, suppose that $\{N(t; s) : t > 0\}$ is a non-homogeneous Poisson process with intensity function $\lambda_s(t)$. We define $\gamma_s : [0, \infty) \to [0, \infty)$ to be the mapping $\gamma_s(t) \equiv \lambda_s(t)$, and let

$$\tilde{t} = \gamma_s^{-1}(t), \tag{2.11}$$

where $\gamma_s^{-1}(t)$ is the generalized inverse of $\lambda_s(t)$. Then $N(\tilde{t}; s)$ has the cumulative intensity function $\Lambda_s(\tilde{t}) = \Lambda_s(\gamma_s^{-1}(t)) = t$, and the independence assumption of $N(\tilde{t}; s)$ and $N(\tilde{t} - \tilde{u}; s)$

for any $0 < \tilde{u} \leq \tilde{t}$ still holds. Therefore, we see that $\{N(\tilde{t}; s) : \tilde{t} > 0\}$ is a homogeneous Poisson process with intensity $\lambda_s = 1$. The significance of this result resides with

$$(\tilde{T}_{1s}, \cdots \tilde{T}_{ks} | N(\tilde{t}; s) = k) \stackrel{d}{=} (\tilde{U}_{(1)}, \cdots, \tilde{U}_{(k)}),$$

where $\tilde{U}_{(j)}$ is the j^{th} order statistic of k independent and identically distributed Uniform$(\tilde{t}^{\lambda}_{1s}, \tilde{t})$ random variables. By working in the modified time scale, we can perform the same exercise as in Chapter 2.2.1, and simplify Equation (2.5) for $\tilde{t} \in [\tilde{t}^{p}_{1s}, \tilde{t}^{p}_{2s}]$ as

$$\begin{aligned} P\left(\tilde{W}_s > \tilde{t} | N(\tilde{t}; s) = k\right) &= \left(1 - p_s \frac{\tilde{t} - \tilde{t}^{p}_{1s}}{\tilde{t} - \tilde{t}^{\lambda}_{1s}}\right)^k \\ &= \tilde{q}_s^k, \end{aligned} \tag{2.12}$$

where $\tilde{q}_s = 1 - p_s(\tilde{t} - \tilde{t}^{p}_{1s})/(\tilde{t} - \tilde{t}^{\lambda}_{1s})$. We can then utilize Equation (2.12) and Definition 2.2.2 to simplify Equation (2.5) with the new time scale as

$$\begin{aligned} P(\tilde{W}_s > \tilde{t}) &= \sum_{k=0}^{\infty} \frac{\tilde{q}_s^k}{k!} \Lambda_s(\tilde{t} - \tilde{t}^{\lambda}_{1s})^k \exp(-\Lambda_s(\tilde{t} - \tilde{t}^{\lambda}_{1s})) \\ &= \exp\left(- \underbrace{\Lambda_s(\tilde{t} - \tilde{t}^{\lambda}_{1s})}_{\tilde{t} - \tilde{t}^{\lambda}_{1s}} p_s \frac{\tilde{t} - \tilde{t}^{p}_{1s}}{\tilde{t} - \tilde{t}^{\lambda}_{1s}} \right) \\ &= \exp(-p_s(\tilde{t} - \tilde{t}^{p}_{1s})). \end{aligned}$$

We then have for any $\tilde{t}$

$$P(\tilde{W}_s > \tilde{t}) = \begin{cases} 1 & \text{if } \tilde{t} < \tilde{t}^{p}_{1s} \\ \exp\left(-p_s(\tilde{t} - \tilde{t}^{p}_{1s})\right) & \text{if } \tilde{t}^{p}_{1s} \leq \tilde{t} \leq \tilde{t}^{p}_{2s} \\ \exp\left(-p_s(\tilde{t}^{p}_{2s} - \tilde{t}^{p}_{1s})\right) & \text{if } \tilde{t}^{p}_{2s} < \tilde{t} \leq T^*. \end{cases} \tag{2.13}$$

Although Equation (2.13) operates in the modified time scale, the main lesson is that we obtained $\{N(\tilde{t}; s) : \tilde{t} > 0\}$ as a homogeneous Poisson process with intensity $\lambda_s = 1$, when we started with $\{N(t; s) : t > 0\}$ as a non-homogeneous Poisson process with intensity $\lambda_s(t)$. By reverting this exercise, we start with a homogeneous Poisson process with intensity $\lambda_s = 1$, and apply the inverse of the time transformation in Equation (2.11) to construct a non-homogeneous Poisson process with intensity $\lambda_s(t)$. Hence, we obtain

$$P(W_s > t) = \begin{cases} 1 & \text{if } t < t^{p}_{1s} \\ \exp\left(-p_s\{\Lambda_s(t) - \Lambda_s(t^{p}_{1s})\}\right) & \text{if } t^{p}_{1s} \leq t \leq t^{p}_{2s} \\ \exp\left(-p_s\{\Lambda_s(t^{p}_{2s}) - \Lambda_s(t^{p}_{1s})\}\right) & \text{if } t^{p}_{2s} < t \leq T^*. \end{cases} \tag{2.14}$$

Similar to Equation (2.10), we can insert Equation (2.14) into Equation (2.4) and obtain the survival function of W as

$$P(W > t) = \begin{cases} 1 & \text{if } t < t_1^p \\ \exp\left(-\left\{\sum_{s\in\mathscr{S}} \lambda_s p_s \left[\Lambda_s(t) I(t \in [t_{1s}^p, t_{2s}^p]) + \Lambda_s(t_{2s}^p) I(t > t_{2s}^p) - \Lambda_s(t_{1s}^p) I(t \geq t_{1s}^p)\right]\right\}\right) & \text{if } t_1^p \leq t \leq T^*, \end{cases} \tag{2.15}$$

and $P(W = \infty) = \prod_{s\in\mathscr{S}} P(W_s > T^*)$ is the probability of zero spot fires occurring passed a fuel break over the time interval $[0, T^*]$, where $t_1^p = \min_{s\in\mathscr{S}}\{t_{1s}^p\}$. As an illustration of Equations (2.14) and (2.15), we now proceed with a few examples.

2.3 Examples

2.3.1 Example 1 - Constant Firebrand Rate Within a Subinterval

Suppose for a fixed $s \in \mathscr{S}$ that the intensity function is $\lambda_s(t) = \lambda_s I(t \in [t_{1s}^\lambda, t_{2s}^\lambda])$ as motivated by Figure A.1a, where $\lambda_s > 0$. We then have for $t \in [t_{1s}^\lambda, t_{2s}^\lambda]$

$$\Lambda_s(t) = \int_0^t \lambda_s(u)du = \int_{t_{1s}^\lambda}^t \lambda_s du = \lambda_s(t - t_{1s}^\lambda),$$

and for any t, we have

$$\Lambda_s(t) = \begin{cases} 0 & \text{if } t < t_{1s}^\lambda \\ \lambda_s(t - t_{1s}^\lambda) & \text{if } t_{1s}^\lambda \leq t \leq t_{2s}^\lambda \\ \lambda_s(t_{2s}^\lambda - t_{1s}^\lambda) & \text{if } t_{2s}^\lambda < T \leq T^*. \end{cases}$$

By recalling that $[t_{1s}^p, t_{2s}^p] \subseteq [t_{1s}^\lambda, t_{2s}^\lambda]$, we insert $\Lambda_s(t)$ into Equation (2.14) to obtain

$$P(W_s > t) = \begin{cases} 1 & \text{if } t < t_{1s}^p \\ \exp\left(-\lambda_s p_s (t - t_{1s}^p)\right) & \text{if } t_{1s}^p \leq t \leq t_{2s}^p \\ \exp\left(-\lambda_s p_s (t_{2s}^p - t_{1s}^p)\right) & \text{if } t_{2s}^p < t \leq T^*, \end{cases}$$

which we recognize as Equation (2.9), as expected. If we were to further suppose that $\lambda_s(t) = \lambda_s I(t \in [t_{1s}^\lambda, t_{2s}^\lambda])$ for every $s \in \mathscr{S}$, then Equation (2.15) simplifies to Equation (2.10).

2.3.2 Example 2 - Power Law Firebrand Rate Within a Subinterval

Suppose for a fixed cell $s \in \mathscr{S}$ that $\lambda_s(t) = \mu_s \lambda_s (\lambda_s[t - t_{1s}^{\lambda}])^{\mu_s - 1} I(t \in [t_{1s}^{\lambda}, t_{2s}^{\lambda}])$ as motivated by Figure A.1b, where $\mu_s > 0$ and $\lambda_s > 0$. We can say for $t \in [t_{1s}^{\lambda}, t_{2s}^{\lambda}]$ that

$$\Lambda_s(t) = \int_0^t \lambda_s(u)du = \int_{t_{1s}^{\lambda}}^t \mu_s \lambda_s (\lambda_s[u - t_{1s}^{\lambda}])^{\mu_s - 1} du = (\lambda_s[t - t_{1s}^{\lambda}])^{\mu_s}.$$

We can then simplify Equation (2.14) as

$$P(W_s > t) = \begin{cases} 1 & \text{if } t < t_{1s}^{p} \\ \exp\left(-\lambda_s^{\mu_s} p_s \{[t - t_{1s}^{\lambda}]^{\mu_s} - [t_{1s}^{p} - t_{1s}^{\lambda}]^{\mu_s}\}\right) & \text{if } t_{1s}^{p} \leq t \leq t_{2s}^{p} \\ \exp\left(-\lambda_s^{\mu_s} p_s \{[t_{2s}^{p} - t_{1s}^{\lambda}]^{\mu_s} - [t_{1s}^{p} - t_{1s}^{\lambda}]^{\mu_s}\}\right) & \text{if } t_{2s}^{p} < t \leq T^*. \end{cases}$$

Remark 1

Observe in the special case where $t_{1s}^{\lambda} = t_{1s}^{p}$, we have

$$P(W_s > t) = \begin{cases} 1 & \text{if } t < t_{1s}^{p} \\ \exp\left(-\lambda_s^{\mu_s} p_s \{[t - t_{1s}^{p}]^{\mu_s}\}\right) & \text{if } t_{1s}^{p} \leq t \leq t_{2s}^{p} \\ \exp\left(-\lambda_s^{\mu_s} p_s \{[t_{2s}^{p} - t_{1s}^{\lambda}]^{\mu_s}\}\right) & \text{if } t_{2s}^{p} < t \leq T^*, \end{cases}$$

which informs us that W_s is a mixture distribution composed of (i) a shifted Weibull distribution with shift parameter t_{1s}^{p}, shape parameter μ_s, and scale parameter $\lambda_s p_s^{-\mu_s}$; and (ii) a point mass distribution at $t = \infty$.

Remark 2

In the special case with $\mu_s = 1$, we then see that Example 2 reduces to Example 1. This result is as expected, since the Exponential distribution is a special case of the Weibull distribution.

2.3.3 Example 3 - Exponential Firebrand Rate Within a Subinterval

For a fixed cell $s \in \mathscr{S}$, suppose that $\lambda_s(t) = \mu_s \exp(\lambda_s[t - t_{1s}^{\lambda}]) I(t \in [t_{1s}^{\lambda}, t_{2s}^{\lambda}])$ as shown in Figure A.1c, where $\mu_s > 0$ and $\lambda_s > 0$. By again considering $t \in [t_{1s}^{\lambda}, t_{2s}^{\lambda}]$, we have

$$\Lambda_s(t) = \int_0^t \lambda_s(u)du = \int_{t_{1s}^{\lambda}}^t \mu_s \exp(\lambda_s[u - t_{1s}^{\lambda}])du = \frac{\mu_s}{\lambda_s}\left(\exp(\lambda_s[t - t_{1s}^{\lambda}]) - 1\right).$$

By inserting $\Lambda_s(t)$ in Equation (2.14), we see that

$$P(W_s > t) = \begin{cases} 1 & \text{if } t < t_{1s}^p \\ \exp\left(-p_s\mu_s/\lambda_s\{\exp(\lambda_s[t - t_{1s}^\lambda]) - \exp(\lambda_s[t_{1s}^p - t_{1s}^\lambda])\}\right) & \text{if } t_{1s}^p \leq t \leq t_{2s}^p \\ \exp\left(-p_s\mu_s/\lambda_s\{\exp(\lambda_s[t_{2s}^p - t_{1s}^\lambda]) - \exp(\lambda_s[t_{1s}^p - t_{1s}^\lambda])\}\right) & \text{if } t_{2s}^p < t \leq T^*. \end{cases}$$

Remark 1

Observe in the special case where $t_{1s}^\lambda = t_{1s}^p$, we have

$$P(W_s > t) = \begin{cases} 1 & \text{if } t < t_{1s}^p \\ \exp\left(-p_s\mu_s/\lambda_s\{\exp(\lambda_s[t - t_{1s}^p])\}\right) & \text{if } t_{1s}^p \leq t \leq t_{2s}^p \\ \exp\left(-p_s\mu_s/\lambda_s\{\exp(\lambda_s[t_{2s}^p - t_{1s}^\lambda])\}\right) & \text{if } t_{2s}^p < t \leq T^*, \end{cases}$$

which informs us that W_s is a mixture distribution composed of (i) a shifted Gompertz distribution with shift parameter t_{1s}^p, shape parameter $\mu_s p_s/\lambda_s$, and scale parameter λ_s; and (ii) a point mass distribution at $t = \infty$.

Chapter 3

Simulation Study

In this Chapter, we simulate the time to the first spot fire that crossed a fuel break in R (R Core Team 2016). The purpose in doing so is to numerically obtain the distribution of W under a variety of situations, and make a comparison with the true distribution of W derived in Chapter 2. The outline of this chapter is as follows. Chapter 3.1 provides preliminaries for the simulation study, and details how spot fires are generated. In order to realistically simulate the time when each cell ignited, Chapter 3.2 presents a stochastic wave propagation fire spread model. We then proceed with three simulation settings in Chapter 3.3, and provide a discussion of the resulting distributions.

3.1 Preliminaries

Analogous to Chapter 2.1, consider an active wildfire over the time interval $[0, T^*]$, where the wildfire ignites at time $t = 0$ within a cell $s \in \mathscr{S}$, $T^* = 45$ is the end of the fire spotting observation window, and $\mathscr{S}$ is the set of cells that can generate firebrands. Throughout the simulation study, we define $\mathscr{S}$ as

$$\mathscr{S} = \{s = [x, x+1] \times [y, y+1] : x \in \{0, \cdots, 10\}, y \in \{-5, \cdots, 5\}\},$$

so that each cell has unit length and width, and at most $|\mathscr{S}| = 121$ cells can generate firebrands within our environment. For each cell $s \in \mathscr{S}$, let $N(t; s)$ denote the cumulative number of firebrands generated by the wildfire within cell s over the time interval $[0, t]$. As in Chapter 2.2, suppose that $\{N(t; s) : t > 0\}$ is a Poisson process with intensity function $\lambda(t; s) = \lambda_s(t)$, and the probability of a firebrand generated within cell s resulting in a spot fire that crossed a fuel break at time t is $p(t; s) = p_s I(t \in [t^p_{1s}, t^p_{2s}])$. Out of simplicity, we set $[t^p_{1s}, t^p_{2s}] = [t^\lambda_{1s}, t^\lambda_{2s}]$, where $[t^\lambda_{1s}, t^\lambda_{2s}]$ is the time interval when cell s can generate firebrands. Within our artificial environment, we designate a set of cells that constitute a fuel break $\mathscr{F}$, in which the wildfire cannot breach without spotting. We specify the fuel break throughout

the simulation study as

$$\mathscr{F} = \{s = [x, x+1] \times [y, y+1] : x \in \{11, 12, 13\}, y \in \{-5, \cdots, 5\}\},$$

so that we have a rectangular fuel break that is three units wide. For a fixed cell $s \in \mathscr{S}$, we simulate

$$M(t; s) = N(t; s) - N(t-1; s) \sim \text{Poisson}\left(\int_{t-1}^{t} \lambda_s(u)du\right)$$

to be the number of firebrands generated by the wildfire within cell s over the time interval $[t-1, t]$. By assuming that firebrands generated within cell s result in a spot fire independently, we simulate the number of spot fires over the time interval $[t-1, t]$ as

$$M^*(t; s) \sim \text{Binomial}(M(t; s), p(t; s)).$$

If $M^*(u; s) = 0$ for $u < t$, but $M^*(t; s) > 0$ for any $s \in \mathscr{S}$, we set $W_s = t$, and obtain $W = \min_{s \in \mathscr{S}}\{W_s\}$ as our simulated realization of the time to the first spot fire. In the event that $M^*(u; s) = 0$ for all $0 \leq u \leq T^*$ and $s \in \mathscr{S}$, we declare that the wildfire did not breach the fuel break, and we set $W = \infty$.

After executing the fire spotting procedure $m = 1{,}000$ times, we estimate $F_W(t)$ with the empirical cumulative distribution function (ECDF)

$$\hat{F}_W(t) = \frac{\sum_{i=1}^{m} I(W^{(i)} \leq t)}{m},$$

where $W^{(i)} \in \{1, 2, \cdots, T^*, \infty\}$ is the i^{th} simulated realization of W. By observing that $\hat{F}_W(t)$ is a sum of independent and identically distributed random variables, such that

$$\begin{aligned} \text{E}(\hat{F}_W(t)) &= F_W(t) \\ \text{Var}(\hat{F}_W(t)) &= \frac{F_W(t)(1 - F_W(t))}{m}, \end{aligned}$$

we can obtain an approximate 95% confidence interval for $F_W(t)$ by the central limit theorem as

$$\left[\hat{F}_W(t) - 1.96\sqrt{\widehat{\text{Var}}(\hat{F}_W(t))}, \hat{F}_W(t) + 1.96\sqrt{\widehat{\text{Var}}(\hat{F}_W(t))}\right],$$

where $\widehat{\text{Var}}(\hat{F}_W(t)) = \hat{F}_W(t)(1 - \hat{F}_W(t))/m$ is a plug-in estimate for $\text{Var}(\hat{F}_W(t))$.

3.2 Wildfire Growth

In order for us to simulate firebrands in a sensible manner, we need to determine $\boldsymbol{t}_1^\lambda = \{t_{1s}^\lambda : s \in \mathscr{S}\}$, which is the set of times when cells $s \in \mathscr{S}$ are ignited. However even under homogeneous conditions, the magnitude and direction of a wildfire's growth over time is stochastic, which means that $\boldsymbol{t}_1^\lambda$ is random. This motivates us to implement a fire growth model to obtain $\boldsymbol{t}_1^\lambda$. Due to the practicality of the wave propagation fire spread model (cf. Richards (1990), Finney (2004), Tymstra *et al.* (2010)), we applied a modified version of PROMETHEUS, initially developed by Han and Braun (2013). This model employs the Canadian Fire Behaviour Prediction system (Forestry Canada, 1992) to obtain empirical rate of spread (RoS) estimates, which are associated with fire growth ellipse parameters. The Canadian Fire Behaviour Prediction system assumes that the RoS has a sigmoidal relationship with the initial spread index (defined below), which is a function of the fuel type, fuel moisture, and wind speed. The envelope of ellipses is then applied to obtain the curve that determines the wildfire, and we specify t_{1s}^λ to be the time when the wildfire curve intersects with cell s.

Specifically, the forward, back, and flank RoS values at time t within cell $s \in \mathscr{S}$ are denoted by $R(t,s)$, $B(t,s)$, and $K(t,s)$, respectively, and they are

$$\log R(t,s) = \log\{\phi_s(1-\exp[-\beta_s I_R(t,s)])^{\nu_s}\} + \varepsilon_R \tag{3.1}$$

$$\log B(t,s) = \log\{\phi_s(1-\exp[-\beta_s I_B(t,s)])^{\nu_s}\} + \varepsilon_B \tag{3.2}$$

$$K(t,s) = \frac{R(t,s)+B(t,s)}{2\rho(\omega)},$$

where ϕ_s, β_s, and ν_s are fuel specific parameters (see Table 6 of Forestry Canada (1992)), $I_R(t,s)$ and $I_B(t,s)$ are the forward and backward initial spread indices, respectively, $\rho(\omega)$ is the length-to-breadth ratio, $\omega = \omega(t,s)$ is the current wind speed at time t within cell s, and $\varepsilon_R, \varepsilon_B \overset{iid}{\sim} \text{Normal}(0, \sigma_\varepsilon^2)$. The purpose of incorporating the error terms ε_R and ε_B in Equations (3.1) and (3.2) is to capture any unexplained variation of the RoS and RoS model, and the log-scale in Equations (3.1) and (3.2) is motivated by a variance-stabilizing transformation in the Han and Braun (2013) analysis. The initial spread indices and length-to-breadth ratio are obtained via empirical estimates

$$I_R(t,s) = \begin{cases} 0.208 g_1(\omega, 0.05039) g_2(r) & \text{if } \omega \le 40 \text{ km/h} \\ 2.496(1-\exp(-0.0818\{\omega-28\}))g_2(r) & \text{if } \omega > 40 \text{ km/h} \end{cases}$$

$$I_B(t,s) = 0.208 g_1(\omega, -0.05039) g_2(r)$$

$$\rho(\omega) = 1 + 8.729\{1-\exp(-0.03\omega)\}^{2.155},$$

where

$$g_1(\omega, x) = \exp(x\omega)$$
$$g_2(r) = 91.9\exp(-0.1386r)\left(1 + \frac{r^{5.31}}{4.93 \times 10^7}\right),$$

and $r = r(t, s)$ is the fuel moisture at time t in cell s; see Forestry Canada (1992) for further details.

By applying the wave propagation concept to the wildfire over $[t-1, t]$, ellipses are generated at each time t with angle of rotation $\theta(t, s)$ to be in the direction of the wind. The resulting parameters for each ellipse are

$$a(t, s) = \frac{R(t, s) + B(t, s)}{2}$$
$$b(t, s) = K(t, s)$$
$$c(t, s) = \frac{R(t, s) - B(t, s)}{2},$$

where $a(t, s)$ and $b(t, s)$ are the major and minor radii parameters, respectively, and $c(t, s)$ is the distance from the left focal point to the centre of the ellipse. Hence, the progression of the wildfire over $[t-1, t]$ is the resulting curve after taking the outer envelope of all the ellipses generated at time t.

3.3 Simulation Settings

3.3.1 Setting 1 - Uniform Firebrand Generation

For our first setting, we consider a special case of Example 1 from Chapter 2.3.1, where we fix $t^{\lambda}_{1s} = 0$ and $t^{\lambda}_{2s} = T^*$ for every $s \in \mathscr{S}$. In other words, firebrands are uniformly generated over cells $s \in \mathscr{S}$ and time $t \in [0, T^*]$. Then for a fixed cell $s \in \mathscr{S}$, the collection of point events $\{N(t; s) : t > 0\}$ is a homogeneous Poisson process with intensity function $\lambda_s(t) = \lambda$, which is constant with respect to both t and s. In order to allow for the probability of a firebrand resulting in a spot fire to vary across cells, we partition $\mathscr{S}$ into three subsets that we refer to as fire zones, and are specified as

$$\mathscr{S}_1 = \{s : x \in \{0, 1, 2, 3\}, y \in \{-5, \cdots, 5\}\}$$
$$\mathscr{S}_2 = \{s : x \in \{4, 5, 6, 7\}, y \in \{-5, \cdots, 5\}\}$$
$$\mathscr{S}_3 = \{s : x \in \{8, 9, 10\}, y \in \{-5, \cdots, 5\}\}.$$

The purpose of these fire zones is that they allow us to specify the probability of a firebrand resulting in a spot fire to be greater, for firebrands generated within cells closer to the

fuel break. That is, we specify $p(t;s) = p_s = \sum_{j=1}^{3} p^{(j)} I(s \in \mathscr{S}_j)$, where $p^{(1)} \leq p^{(2)} \leq p^{(3)}$. As an illustration of our fire spotting process within our simulated environment, consider the case where $\lambda = 0.05$, and $p^{(1)} = p^{(2)} = p^{(3)} = 0.007$ in Figure A.2. The left panel illustrates $N(t;s)$ for every $s \in \mathscr{S}$ over the time interval $[0, 19]$, and the right panel exhibits that every $s \in \mathscr{S}$ can generate firebrands at time $t = 19$. Furthermore, cells $s \in \mathscr{F}$ are coloured dark blue to represent the three unit wide rectangular fuel break that the wildfire is attempting to breach. By increasing time by one unit to $t = 20$, Figure A.2b illustrates that cell $s = [4, 5] \times [-1, 0]$ is coloured red, which indicates that $M^*(20; s) > 0$. This means that we set $W_s = 20$, and since this is the first occurrence of a spot fire, we declare $t = 20$ as a simulated realization of W. An equivalent narrative is presented in Figure A.3, where $\lambda = 0.05$, $p^{(1)} = 0.007$, $p^{(2)} = 0.010$, and $p^{(3)} = 0.015$. We see that $M^*(18; s) > 0$ for $s = [6, 7] \times [-2, -1]$, so that $t = 18$ is a simulated realization of W.

After obtaining 1,000 simulated realizations of W, we want to compare the simulated distribution of W with its theoretical counterpart that we derived in Chapter 2. From Equation (2.9), the survival function of W_s for each $s \in \mathscr{S}$ is

$$P(W_s > t) = \begin{cases} 1 & \text{if } t < 0 \\ \exp\left(-\lambda p_s t\right) & \text{if } 0 \leq t \leq T^*, \end{cases} \tag{3.3}$$

so that Equation (3.3) is the survival function of an Exponential random variable with rate λp_s for $t \in [0, T^*]$. Since we assigned $W_s = \infty$ if none of the firebrands generated within cell s resulted in a spot fire by time $t = T^*$, we have $P(W_s = \infty) = P(W_s > T^*)$. Hence, we make use of Equation (2.10) and obtain the survival function of W as

$$P(W > t) = \begin{cases} 1 & \text{if } t < 0 \\ \exp\left(-\sum\limits_{s \in \mathscr{S}} \lambda p_s t\right) & \text{if } 0 \leq t \leq T^*, \end{cases}$$

and $P(W = \infty) = \prod\limits_{s \in \mathscr{S}} P(W_s > T^*)$. Under this particular setting, we can recognize W as a mixture distribution composed of (i) an Exponential random variable with rate $\sum\limits_{s \in \mathscr{S}} \lambda_s p_s$, and (ii) a point mass distribution at $t = \infty$.

Although the distribution of W in this setting is well-known, this may not be the case in more complex settings. In order to gain investigate the distribution of W, we compute the hazard function of W, which is the instantaneous rate of a spot fire occurring. The hazard function for this setting is

$$h_W(t) = \frac{f_W(t)}{P(W > t)} = \lambda \sum_{j=1}^{3} p^{(j)} |\mathscr{S}_j|, \tag{3.4}$$

where $f_W(t)$ is the density function of W, and $|\mathscr{S}_j|$ is the number of cells in fire zone j. We can see from Equation (3.4) that the occurrence of a spot fire is constant, with respect to time, which should not come as a surprise since the Exponential distribution is memoryless.

Figure A.4 plots the ECDF accompanied with $F_W(t)$ and a histogram of the simulated realizations of W for the two cases illustrated in Figures A.2 and A.3, where we applied a continuity correction factor to W. We can see that the ECDF is in close agreement with the true distribution function, as the true distribution function resides in the 95% confidence interval for all $t \in [0, T^*]$. Furthermore, we can clearly see within the histograms that W follows a mixture distribution composed of (i) an Exponential distribution and (ii) a point mass distribution at $t = \infty$. By comparing these two cases, we can see that the probability of observing a spot fire is higher with the parameter settings of Figure A.3 as opposed to Figure A.2. This result is as expected, since the probability of a firebrand resulting in a spot fire is higher within two fire zones. Table 3.1 presents the simulated probability of a spot fire not occurring, under a variety of parameter settings. The same conclusions apply for all of the parameter settings, since the true probability resides in the 95% confidence interval. Additional plots for the parameter settings presented in Table 3.1 can be found in Figures B.1 and B.2 in Appendix B.

Table 3.1: Parameter settings along with the simulated probability, 95% confidence interval (CI), and true probability of a spot fire not crossing the fuel break. The two cases in Figure A.4 are presented in bold font.

λ	$p^{(1)}$	$p^{(2)}$	$p^{(3)}$	$\hat{\mathrm{P}}(W = \infty)$	95 % CI	$\mathrm{P}(W = \infty)$
0.002	0.05	0.08	0.15	0.394	[0.364, 0.424]	0.383
0.002	0.15	0.15	0.15	0.206	[0.181, 0.231]	0.195
0.002	0.15	0.20	0.25	0.124	[0.104, 0.144]	0.119
0.05	0.001	0.007	0.02	0.114	[0.094, 0.134]	0.103
0.05	**0.007**	**0.007**	**0.007**	**0.154**	**[0.132, 0.176]**	**0.149**
0.05	**0.007**	**0.010**	**0.015**	**0.060**	**[0.045, 0.075]**	**0.061**
0.10	0.0025	0.0025	0.0025	0.240	[0.214, 0.266]	0.256
0.85	0.0002	0.0002	0.0002	0.394	[0.364, 0.424]	0.396

3.3.2 Setting 2 - Cells Ignited By Zone

For our second setting, we consider another special case of Example 1 from Chapter 2.3.1, where we used a deterministic cellular automaton fire growth model to obtain $\boldsymbol{t}_1^{\lambda}$. That is, we no longer fix $t_{1s} = 0$ and $t_{2s} = T^*$ for every $s \in \mathscr{S}$, but rather, t_{1s} and t_{2s} are fixed to separate times to roughly mimic fire growth. This means for a fixed cell $s \in \mathscr{S}$, the collection of point events $\{N(t; s) : t > 0\}$ is a non-homogeneous Poisson process with

intensity function $\lambda_s(t) = \lambda_s I(t \in [t^\lambda_{1s}, t^\lambda_{2s}])$, where

$$
\begin{aligned}
t^\lambda_{1s} &= \sum_{i=1}^{3} t^{(i)} I(s \in \mathscr{S}^i) \\
\lambda_s &= \sum_{i=1}^{3} \lambda^{(i)} I(s \in \mathscr{S}^i) \\
\mathscr{S}^1 &= \{s \in \mathscr{S} : x \in \{0,1,2,3\}, y \in \{-1,0,1\}\} \\
\mathscr{S}^2 &= \{s \in \mathscr{S} : x \in \{0,\cdots,6\}, y \in \{-3,\cdots,3\}, s \notin \mathscr{S}^1\} \\
\mathscr{S}^3 &= \mathscr{S} \backslash \{\mathscr{S}^1 \bigcup \mathscr{S}^2\},
\end{aligned}
$$

and $t^{(1)} = 5$, $t^{(2)} = 15$, and $t^{(3)} = 25$ are fixed. We also considered two separate conditions for t^λ_{2s}:

(i) Cells $s \in \mathscr{S}$ only generate firebrands for 20 time units, meaning that $t^\lambda_{2s} = t^\lambda_{1s} + 20$. This can be interpreted as each cell s becoming extinguished after 20 time units from being ignited.

(ii) Cells $s \in \mathscr{S}$ continue to generate firebrands until $t = T^*$, so that $t^\lambda_{2s} = T^*$.

As for the probability of a firebrand resulting in a spot fire, we maintained with the same specification of $p(t;s)$ as in Setting 1, so that $p(t;s) = \sum_{j=1}^{3} p^{(j)} I(s \in \mathscr{S}_j)$. Figures A.5 and A.6 present two separate cases of cells generating firebrands with $t^\lambda_{2s} = t^\lambda_{1s} + 20$. Similar to Setting 1, Figure A.5b shows us that $t = 36$ is a simulated realization for W, whereas $t = 25$ is a simulated realization for W in Figure A.6b.

Similar to Setting 1, the survival function of W_s for a fixed cell $s \in \mathscr{S}$ is

$$
P(W_s > t) = \begin{cases} 1 & \text{if } t < t^\lambda_{1s} \\ \exp\left(-\lambda_s p_s (t - t^\lambda_{1s})\right) & \text{if } t^\lambda_{1s} \le t \le t^\lambda_{2s}, \end{cases}
$$

which informs us that for $t \in [0, T^*]$, W_s is an Exponential random variable with rate $\lambda_s p_s$ and shift parameter t^λ_{1s}. We can then obtain the survival function of W as

$$
P(W > t) = \begin{cases} 1 & \text{if } t < 5 \\ \exp\left(-\left\{\sum_{s \in \mathscr{S}} \lambda_s p_s \left[t I(t \in [t^\lambda_{1s}, t^\lambda_{2s}]) + t^\lambda_{2s} I(t > t^\lambda_{2s}) - t^\lambda_{1s} I(t \ge t^\lambda_{1s})\right]\right\}\right) & \text{if } 5 \le t \le T^*, \end{cases}
$$

and $P(W = \infty) = \prod_{s \in \mathscr{S}} P(W_s > T^*)$.

Based on the way we specified $[t_{1s}^{\lambda}, t_{2s}^{\lambda}]$, the hazard function of W for this setting is

$$h_W(t) = \begin{cases} \lambda^{(1)} p^{(1)} |\mathscr{S}^1 \cap \mathscr{S}_1| & \text{if } 5 < t \leq 15 \\ \sum_{i=1}^{2} \sum_{j=1}^{2} \lambda^{(i)} p^{(j)} |\mathscr{S}^i \cap \mathscr{S}_j| & \text{if } 15 < t \leq 25 \\ \sum_{i=1}^{3} \sum_{j=1}^{3} \lambda^{(i)} p^{(j)} |\mathscr{S}^i \cap \mathscr{S}_j| & \text{if } 25 < t \leq 45 \\ 0 & \text{otherwise,} \end{cases}$$

if $t_{2s}^{\lambda} = T^*$, and

$$h_W(t) = \begin{cases} \lambda^{(1)} p^{(1)} |\mathscr{S}^1 \cap \mathscr{S}_1| & \text{if } 5 < t \leq 15 \\ \sum_{i=1}^{2} \sum_{j=1}^{2} \lambda^{(i)} p^{(j)} |\mathscr{S}^i \cap \mathscr{S}_j| & \text{if } 15 < t \leq 25 \\ \sum_{i=1}^{2} \sum_{j=1}^{2} \lambda^{(i)} p^{(j)} |\mathscr{S}^i \cap \mathscr{S}_j| & \text{if } 25 < t \leq 45 \\ \sum_{i=2}^{3} \sum_{j=1}^{2} \lambda^{(i)} p^{(j)} |\mathscr{S}^i \cap \mathscr{S}_j| & \text{if } 25 < t \leq 35 \\ \lambda^{(3)} \sum_{j=1}^{2} p^{(j)} |\mathscr{S}^3 \cap \mathscr{S}_j| & \text{if } 35 < t \leq 45 \\ 0 & \text{otherwise,} \end{cases}$$

if $t_{2s}^{\lambda} = t_{1s}^{\lambda} + 20$. In either scenario, we can see that the hazard function is a step-function, so that the rate of a spot fire occurrence is piece-wise constant. Furthermore, each step of the hazard function occurs whenever a cell transitions to a new state.

Figure A.7 plots the ECDF and distribution function of W in the left panel and the histogram of W in the right panel, for the two cases presented in Figures A.5 and A.6. We can see the effect of cells changing states within these two plots, which is precisely what $h_W(t)$ informs us. Similar to Table 3.1, we present the probability of a firebrand resulting in a spot fire, and its true value under a variety of parameter settings in Table 3.2. We see that the true probability values reside in their 95% confidence intervals, minus one case that narrowly misses. Additional plots for the parameter settings presented in Table 3.2 can be found in Figures B.3 and B.4 in Appendix B.

3.3.3 Setting 3 - Cells Ignited According to a Fire Growth Model

For our third setting, we used the Han and Braun (2013) stochastic fire growth model as discussed in Chapter 3.2 to obtain $\boldsymbol{t}_1^{\lambda}$. In order to do so, assumptions need to be made pertaining to the environment where the wildfire is burning. For the sake of simplicity, we assume a spatial homogeneous environment, in terms of fuel type, wind speed and direction, and fuel moisture; but the wind speed and fuel direction can vary across each simulation. We designate the fuel type to be mature jack or lodgepole pine (C-3 in Forestry Canada

Table 3.2: Parameter settings along with the simulated probability, 95% confidence interval (CI), and true probability of a spot fire not crossing the fuel break. The two cases in Figure A.7 are presented in bold font.

$\lambda^{(1)}$	$\lambda^{(2)}$	$\lambda^{(3)}$	$p^{(1)}$	$p^{(2)}$	$p^{(3)}$	t_{2s}^{λ}	$\hat{P}(W=\infty)$	95% CI	$P(W=\infty)$
0.05	0.05	0.05	0.007	0.007	0.007	45	0.326	[0.297, 0.355]	0.346
0.05	0.05	0.05	0.007	0.007	0.007	$t_{1s}^{\lambda}+20$	0.419	[0.388, 0.450]	0.429
0.05	0.05	0.05	0.007	0.010	0.015	45	0.220	[0.175, 0.225]	0.226
0.05	0.05	0.05	0.007	0.010	0.015	$t_{1s}^{\lambda}+20$	0.282	[0.254, 0.310]	0.289
0.05	0.10	0.07	0.007	0.007	0.007	45	0.189	[0.165, 0.213]	0.192
0.05	**0.10**	**0.07**	**0.007**	**0.007**	**0.007**	$\boldsymbol{t_{1s}^{\lambda}+20}$	**0.285**	**[0.257, 0.313]**	**0.270**
0.05	0.10	0.07	0.007	0.010	0.015	45	0.095	[0.077, 0.113]	0.100
0.05	**0.10**	**0.07**	**0.007**	**0.010**	**0.015**	$\boldsymbol{t_{1s}^{\lambda}+20}$	**0.152**	**0.130, 0.174**	**0.150**

(1992)), so that $\phi_s = 110$, $\beta_s = 0.0444$, and $\nu_s = 3$ are the fuel specific parameters of Equations (3.1) and (3.2). The reason why we specified this fuel is simply due to the perception of pine cones and other foliage becoming firebrands that can result in a spot fire. As for the error terms ε_R and ε_B in Equations (3.1) and (3.2), we set $\sigma_\varepsilon^2 = 0.4^2$ to account for the unexplained variation not explained by the model. All that remains for us to obtain the RoS values are the wind speed and fuel moisture. Since we assumed a spatially homogeneous environment, this means that the fuel moisture and wind speed only vary over time. Due to the perceived autocorrelation within these variables, we generate fuel moisture and wind speed as independent autoregressive models of order two

$$r(t) = \mu_r + \varphi_1 r(t-1) + \varphi_2 r(t-2) + \varepsilon_r,$$
$$\omega(t) = \mu_\omega + \psi_1 \omega(t-1) + \psi_2 \omega(t-2) + \varepsilon_\omega,$$

where $\mu_r = 25$, $\varphi_1 = 0.7$, $\varphi_2 = 0.25$, $\varepsilon_r \sim \text{Normal}(0, \sigma_r^2)$, $\sigma_r^2 = 0.85^2$, $\mu_\omega = 28$, $\psi_1 = 0.45$, $\psi_2 = 0.15$, $\varepsilon_\omega \sim \text{Normal}(0, \sigma_\omega^2)$, and $\sigma_\omega^2 = 2.45^2$. By igniting the fire at time $t = 0$ as a point ignition at location $(0.5, 0.5)$, we generate the wildfire over times $t \in \{1, 2, \cdots, T^*\}$. We also specify $\theta(t, s) = 0$, for all s and t, so that the wind is constantly gusting eastwards.

In terms of generating firebrands, we have the collection of point events $\{N(t; s) : t > 0\}$ as a non-homogeneous Poisson process with intensity function $\lambda_s(t) = \lambda_s I(t \in [t_{1s}^{\lambda}, t_{2s}^{\lambda}])$, for each $s \in \mathscr{S}$. To make comparisons with Setting 2, we continue to specify the firebrand rate as $\lambda_s = \sum_{i=1}^{3} \lambda^{(i)} I(s \in \mathscr{S}^i)$. However, we specify $p(t; s) = p_s I(t \in [t_{1s}^{\lambda}, t_{2s}^{\lambda}])$, where $p_s = \kappa\lceil x \rceil/(11+3)$ for some $\kappa > 0$, so that p_s is proportional to the distance from the end of cell s to the end of the three unit wide fuel break.

Figure A.8 illustrates cells generating firebrands, where we set $t_{2s}^{\lambda} = t_{1s}^{\lambda} + 20$. With this example, we can see the wildfire spreading eastwards, and roughly takes on an elliptical shape. For this case, we can see that the first spot fire occurs at time $t = 27$ within cell $s = [7, 8] \times [3, 4]$. Since we did not prespecify $\boldsymbol{t}_1^{\lambda}$, we can branch off into two separate

situations: (i) we fix $\boldsymbol{t}_1^\lambda$ to a simulated realization from the fire growth model, and (ii) we let $\boldsymbol{t}_1^\lambda$ vary across simulations. We consider both of these subcases below.

Fixed $\mathbf{t}_1^\lambda$

Upon simulating the wildfire once to obtain a simulated realization of $\boldsymbol{t}_1^\lambda$, we then proceeded to simulate the firebrand generation process 1,000 times. That is, we generated realizations of W conditional on $\boldsymbol{t}_1^\lambda$ to obtain $F_{W|\boldsymbol{t}_1^\lambda}(t)$. This can be interpreted as the distribution of W conditional on a particular wildfire. Figure A.9 plots a simulated realization of $\boldsymbol{t}_1^\lambda$, in which we can see the progression of the wildfire over time. Furthermore, there are cells $s \in \mathscr{S}$ where $t_{1s}^\lambda > T^*$, so that not every cell can generate firebrands over $[0, T^*]$.

Since $\boldsymbol{t}_1^\lambda$ is constant across the 1,000 simulations, we can compare the ECDF to the true conditional distribution function that we derived in Chapter 2. The true conditional survival function for W_s in this setting is

$$P(W_s > t|\boldsymbol{t}_1^\lambda) = \begin{cases} 1 & \text{if } t < t_{1s}^\lambda \\ \exp\left(-\lambda_s p_s (t - t_{1s}^\lambda)\right) & \text{if } t_{1s}^\lambda \leq t \leq t_{2s}^\lambda, \end{cases}$$

and the conditional survival function of W is

$$P(W > t|\boldsymbol{t}_1^\lambda) = \begin{cases} 1 & \text{if } t < 0 \\ \exp\left(-\left\{\sum_{s\in\mathscr{S}} \lambda_s p_s \left[tI(t \in [t_{1s}^\lambda, t_{2s}^\lambda]) + t_{2s}^\lambda I(t > t_{2s}^\lambda) - t_{1s}^\lambda I(t \geq t_{1s}^\lambda)\right]\right\}\right) & \text{if } 0 \leq t \leq T^*, \end{cases}$$

which we recognize has the same structure as Setting 2. We can obtain the conditional hazard function of W for this setting as

$$h_{W|\boldsymbol{t}_1^\lambda}(t) = \begin{cases} \sum_{s\in\mathscr{S}} \lambda_s p_s I(t \in [t_{1s}^\lambda, t_{2s}^\lambda]) & \text{if } 0 < t \leq T^* \\ 0 & \text{otherwise,} \end{cases}$$

so that $h_{W|\boldsymbol{t}_1^\lambda}(t)$ is a step function where the steps occur whenever cell s transitions to a new state.

Figure A.10 plots the distribution of W, given $\boldsymbol{t}_1^\lambda$, for both the parameter settings in Figure A.8, and the parameter settings in Figure A.8 with $t_{2s}^\lambda = T^*$. We can see that these two cases are quite similar, except it is more likely for a spot fire to occur when $t_{2s}^\lambda = T^*$. We can further compare Figures A.7 and A.10, and see that the distribution function of Figure A.10 is quite smooth compared to Figure A.7. This is simply due to $h_{W|\boldsymbol{t}_1^\lambda}(t)$ taking several steps, and each step is less profound compared to $h_W(t)$ from Setting 2. Table 3.3 presents the simulated and true probability of a spot fire not occurring, which aside from two cases, we see that the true probability resides within the 95% confidence interval.

Additional plots for the parameter settings presented in Table 3.3 can be found in Figures B.5 and B.6 in Appendix B.

Table 3.3: Parameter settings along with the simulated probability, 95% confidence interval (CI), and true probability of a spot fire not crossing the fuel break. The two cases in Figure A.10 are presented in bold font.

$\lambda^{(1)}$	$\lambda^{(2)}$	$\lambda^{(3)}$	κ	t_{2s}^{λ}	$\hat{P}(W=\infty\|\boldsymbol{t}_1^{\lambda})$	95% CI	$P(W=\infty\|\boldsymbol{t}_1^{\lambda})$
0.05	0.05	0.05	0.05	T^*	0.046	[0.033, 0.059]	0.062
0.05	0.05	0.05	0.05	$t_{1s}^{\lambda}+20$	0.151	[0.129, 0.173]	0.170
0.05	0.05	0.05	0.08	T^*	0.005	[0.001, 0.009]	0.012
0.05	0.05	0.05	0.08	$t_{1s}^{\lambda}+20$	0.059	[0.044, 0.074]	0.059
0.05	**0.10**	**0.07**	**0.05**	$\boldsymbol{T^*}$	**0.011**	**[0.005, 0.017]**	**0.013**
0.05	**0.10**	**0.07**	**0.05**	$\boldsymbol{t_{1s}^{\lambda}+20}$	**0.061**	**[0.046, 0.076]**	**0.064**
0.05	0.10	0.07	0.08	T^*	0	NA	0.001
0.05	0.10	0.07	0.08	$t_{1s}^{\lambda}+20$	0.01	[0.004, 0.016]	0.012

Varying $\mathbf{t}_1^{\lambda}$

For this subsetting, we jointly simulate the fire growth model and firebrand generation process to obtain our realizations of W. Since $\boldsymbol{t}_1^{\lambda}$ is random, we cannot use Equation (2.15) to obtain the survival function of W. However, upon conditioning on $\boldsymbol{t}_1^{\lambda}$, we have

$$F_W(t) = \int F_W(t|\boldsymbol{t}_1^{\lambda}) f(\boldsymbol{t}_1^{\lambda}) d\boldsymbol{t}_1^{\lambda} \tag{3.5}$$

$$= \mathrm{E}\{F_W(t|\boldsymbol{t}_1^{\lambda})\}. \tag{3.6}$$

where $F_W(t|\boldsymbol{t}_1^{\lambda})$ is the conditional distribution function of W, which we are familiar with, and $f(\boldsymbol{t}_1^{\lambda})$ is the joint density of $\boldsymbol{t}_1^{\lambda}$. Although we can in principle obtain $F_W(t)$, it is very difficult to carry out the expectation of Equation (3.6) since $f(\boldsymbol{t}_1^{\lambda})$ is difficult to obtain. However, since we are very familiar with $F_W(t|\boldsymbol{t}_1^{\lambda})$, it is more sensible to approximate $F_W(t)$ as

$$\tilde{F}_W(t) = \frac{1}{m}\sum_{i=1}^{m} F_W(t|\{\boldsymbol{t}_1^{\lambda}\}^{(i)}),$$

where $F_W(t|\{\boldsymbol{t}_1^{\lambda}\}^{(i)})$ is the conditional distribution of W for the i^{th} simulation. Figure A.11 plots the histogram and ECDF accompanied with $\tilde{F}_W(t)$ for the same parameter settings as in Figure A.10, and we see that the ECDF is in agreement with $\tilde{F}_W(t)$. By comparing Figure A.11 with Figure A.10, we can see that they are quite similar. This is in due to the 1,000 simulated wildfires being similar. In other words, we can expect contrasts between the distribution of W and $W|\boldsymbol{t}_1^{\lambda}$ if the simulated wildfires are diverse. Table 3.4 presents the simulated and true probability of a spot fire not occurring, where we see that the true probability resides within the 95% confidence interval, except for one case. Additional plots

for the parameter settings presented in Table 3.4 can be found in Figures B.7 and B.8 in Appendix B.

Table 3.4: Parameter settings along with the simulated probability, 95% confidence interval (CI), and true probability of a spot fire not crossing the fuel break. The two cases in Figure A.11 are presented in bold font.

$\lambda^{(1)}$	$\lambda^{(2)}$	$\lambda^{(3)}$	κ	t_{2s}^{λ}	$\hat{P}(W=\infty)$	95% CI	$P(W=\infty)$
0.05	0.05	0.05	0.05	T^*	0.065	[0.050, 0.080]	0.061
0.05	0.05	0.05	0.05	$t_{1s}^{\lambda}+20$	0.133	[0.112, 0.154]	0.148
0.05	0.05	0.05	0.08	T^*	0.013	[0.006, 0.020]	0.126
0.05	0.05	0.05	0.08	$t_{1s}^{\lambda}+20$	0.041	[0.029, 0.053]	0.049
0.05	**0.10**	**0.07**	**0.05**	$\boldsymbol{T^*}$	**0.012**	**[0.005, 0.019]**	**0.014**
0.05	**0.10**	**0.07**	**0.05**	$\boldsymbol{t_{1s}^{\lambda}+20}$	**0.035**	**[0.024, 0.046]**	**0.054**
0.05	0.10	0.07	0.08	T^*	0.001	[0, 0.003]	0.001
0.05	0.10	0.07	0.08	$t_{1s}^{\lambda}+20$	0.001	[0, 0.003]	0.001

Chapter 4

Conclusion

4.1 Summary

In this project, we used a counting process framework to derive distributions of the time to the first spot fire that crossed a fuel break, under numerous scenarios. Two specifications are fundamental towards deriving the distributions, namely the rate at which firebrands are emitted from the wildfire, and the probability that a firebrand results in a spot fire that surpassed a fuel break. By using a Poisson process and specifying a simple form for the probability of a firebrand to result in a spot fire, we showed that the derived distributions follow a mixture distribution, with the Exponential, Weibull, and Gompertz distributions arise as a component of the mixture distribution under special circumstances. We simulated the time to the first spot fire, where our results corroborate with the derived distributions. We also implemented a wildfire simulator to showcase how our fire spotting mechanism can be implemented in practice.

The derived distributions can assist fire managers to prepare for the occurrence of a wildfire breaching a fuel break. In particular, this can aid fire crews to attempt to extinguish a spot fire that breached a fuel break, before the fire becomes out-of-control. Furthermore, we showed that the true probability of a spot fire occurring by time t resides within the 95% confidence intervals through our simulation study. This allows us to provide fire managers with an interval estimate for the true probability of a spot fire of interest occurring.

4.2 Future Investigation

Although our derived distributions can assist fire managers, there are a variety of issues that should be addressed to further enhance the value of this research. One such matter pertains to the firebrand and probability parameters used within the simulation study, as these quantities are unknown and need to be estimated. However, the challenge within our context is that many of the firebrands generated by the wildfire are unobserved due to their

extinguishment. One approach to overcome this challenge is to solely focus our attention towards estimating the rate at which spot fires breach a fuel break.

We also assumed that firebrands generated within a particular cell are independent from each other, and that the times to the first spot fire within each cell are independent from each other. The firebrand independent condition was imposed on us due to employing a Poisson process for the number of firebrands generated by the wildfire within a cell. This can be overcome by alternatively considering a non-Poisson counting process that utilizes the history of firebrand generation. For the time to the first spot fire for each cell independence, we can either consider specifying the spatial correlation within $p(t; s)$, or directly model the joint distribution of the W_s's.

Throughout this project, we stratified the environment into cells in order to generate spot fires, and simulated W in discrete time in Chapter 3. This requires the researcher to not only specify the dimensions and shape of each cell, but the set of time units for fire growth and firebrand generation. Ultimately, our objective is to expand our derivations to embody a continuous spatio-temporal process so that our model can be utilized in real time.

We also derived the marginal distribution of W throughout this project, however this does not show the dependence of W with risk factors, such as fuel type, wind speed, etc. In other words, there is a vector of covariates $\boldsymbol{z}_s$ that is associated with W. This would motivate the investigation of the conditional distribution of W, given $\boldsymbol{z}_s$. This can allow us to make predictions for the likelihood of observing a spot fire, given the risk factors associated with fire spotting, and further strengthen fire management fighting wildfires.

Bibliography

Albini, F. A. (1979). Spot fire distance from burning trees – a predictive model. Technical report. INT-56, USDA Forest Service. Ogden, Utah.

Boychuk, D., W. J. Braun, R.J. Kulperger, Z.L. Krougly and D. A. Stanford (2008). A stochastic forest fire growth model. *Environmental and Ecological Statistics* **16**(2), 133–151.

Cox, D. R. and V. Isham (1980). *Point Processes*. Chapman and Hall.

Finney, M. A. (2004). FARSITE: Fire area simulator-model development and evaluation. Technical report. U.S. Department of Agriculture, Forest Service, Rocky Mountain Research Station. Ogden, Utah.

Forestry Canada Fire Danger Group (1992). Development and structure of the Canadian forest fire behaviour prediction system. Technical report. ST-X-3, Forestry Canada. Ottawa, Ontario.

Ha, T. T. (2016). A perfect storm of conditions: Here's how the blaze reached Fort McMurray, and why it spread so fast. *The Globe and Mail*.

Han, L. and W. J. Braun (2013). Dionysus: a stochastic fire growth scenario generator. *Environmetrics* **25**(6), 431–442.

Martin, J. and T. Hillen (2016). The spotting distribution of wildfires. *Applied Sciences* **6**(6), 177–211.

Perryman, H. A., C. J. Dugaw, M. Varner and D. L. Johnson (2013). A cellular automata model to link surface fires to firebrand lift-off and dispersal. *International Journal of Wildland Fire* **22**(4), 428–439.

R Core Team (2016). *R: A Language and Environment for Statistical Computing*. R Foundation for Statistical Computing. Vienna, Austria.

Richards, G. D. (1990). An elliptical growth model of forest fire fronts and its numerical solution. *International Journal for Numerical Methods in Engineering* **30**, 1163–1179.

Snowdon, W. (2016). Fort McMurray wildfire costliest insured disaster in Canadian history. *CBC News*.

Thomas, P. A. and R. S. McAlpine (2010). *Fire in the Forest*. Cambridge University Press.

Tymstra, C. R., W. Bryce, B. M. Wotton, S. W. Taylor and O. B. Armitage (2010). Development and structure of Prometheus, the Canadian wildland fire growth simulation model. Technical report. NOR-X-417, Natural Resources Canada, Canadian Forest Service, Northern Forestry Centre. Edmonton, Alberta.

Appendix A

List of Figures

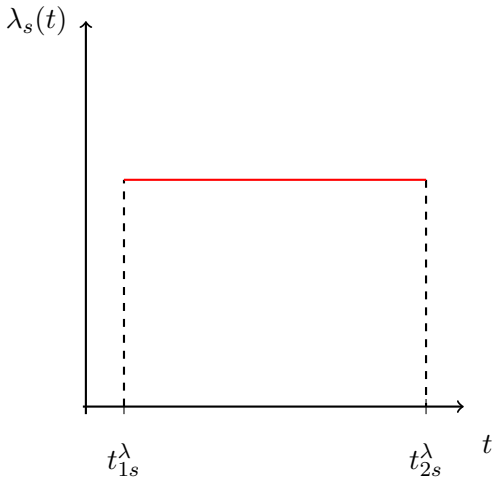

(a) $\lambda_s(t) = \lambda_s I(t \in [t^{\lambda}_{1s}, t^{\lambda}_{2s}])$.

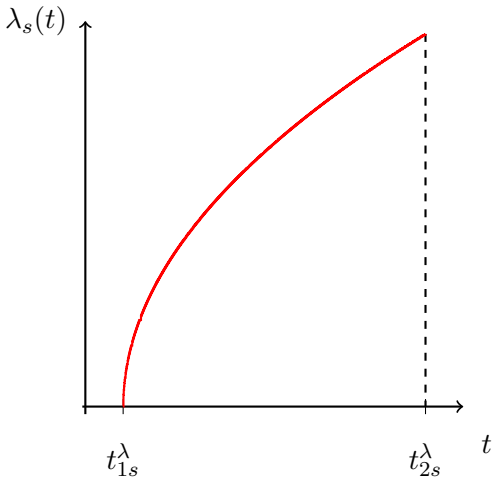

(b) $\lambda_s(t) = \mu_s \lambda_s (\lambda_s [t - t^{\lambda}_{1s}])^{\mu_s - 1} I(t \in [t^{\lambda}_{1s}, t^{\lambda}_{2s}])$.

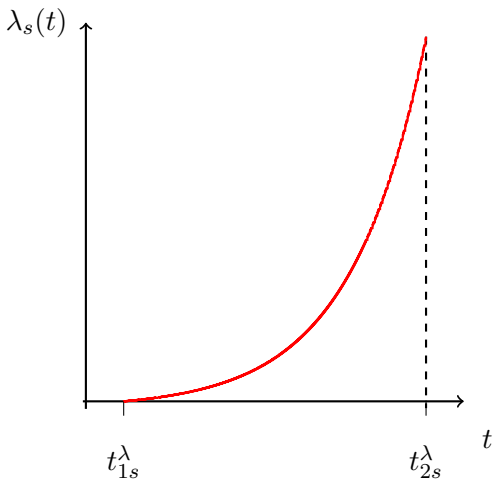

(c) $\lambda_s(t) = \mu_s \exp(\lambda_s [t - t^{\lambda}_{1s}]) I(t \in [t^{\lambda}_{1s}, t^{\lambda}_{2s}])$.

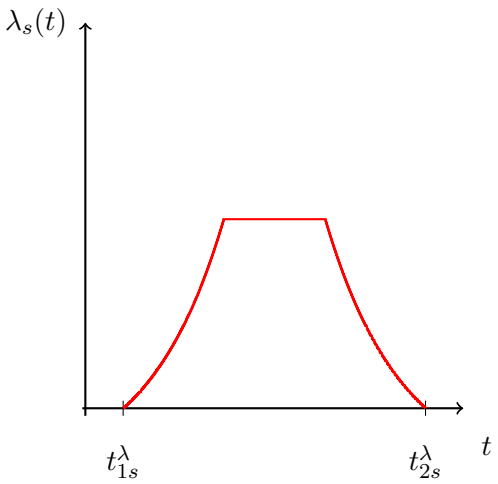

(d) $\lambda_s(t)$ is a piece-wise defined function.

Figure A.1: Examples of $\lambda_s(t)$ that can arise in practice.

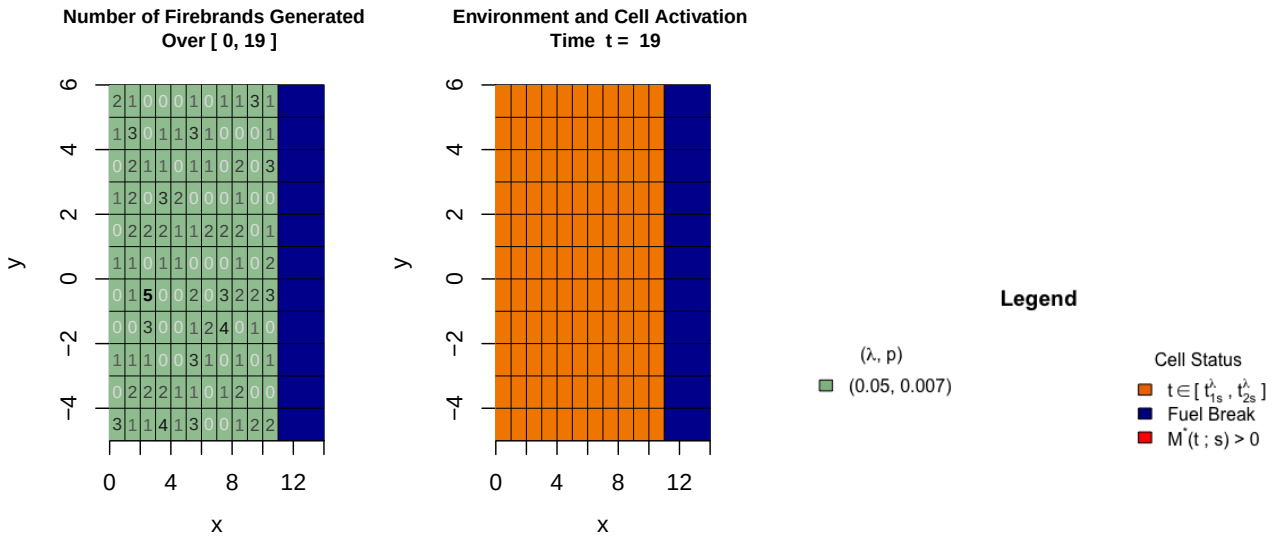

(a) All firebrands generated within cells $s \in \mathscr{S}$ have failed to result in a spot fire that crossed the fuel break.

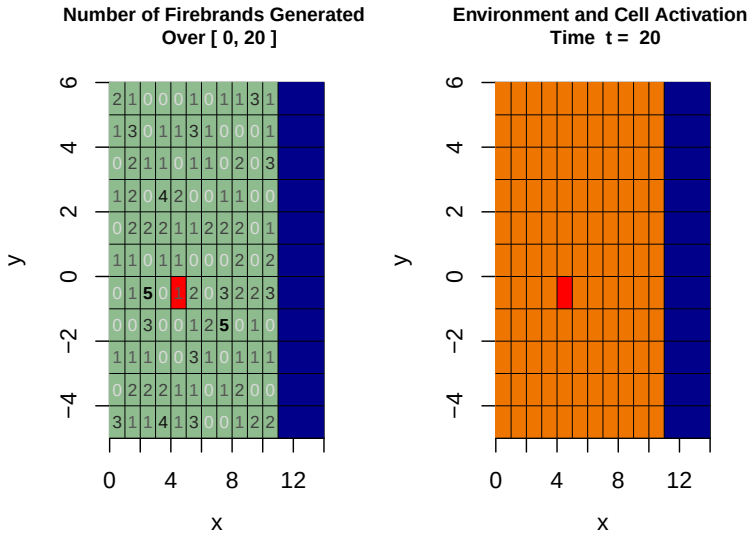

(b) A firebrand generated within cell $s = [4, 5] \times [-1, 0]$ results in a spot fire that crossed the fuel break.

Figure A.2: An illustration of the fire spotting procedure, where the left panel shows $N(t; s)$ for each $s \in \mathscr{S}$ over the time interval $[0, t]$, and the right panel illustrates the state of each cell.

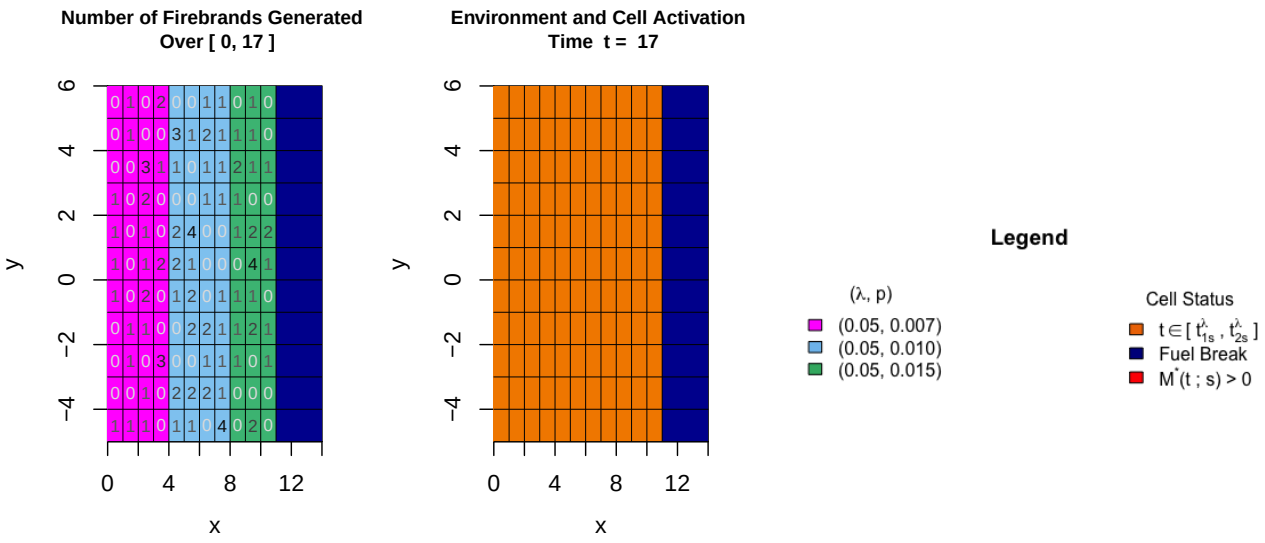

(a) All firebrands generated within cells $s \in \mathscr{S}$ have failed to result in a spot fire that crossed the fuel break.

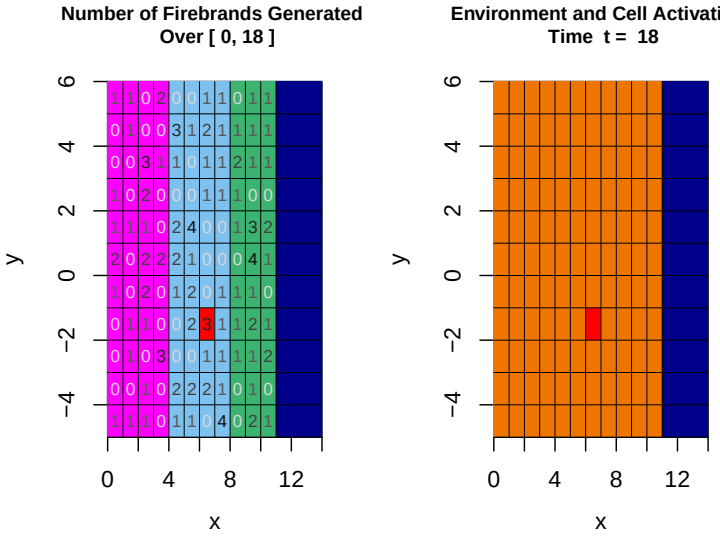

(b) A firebrand generated within cell $s = [6, 7] \times [-2, -1]$ results in a spot fire that crossed the fuel break.

Figure A.3: An illustration of the fire spotting procedure, where the left panel shows $N(t; s)$ for each $s \in \mathscr{S}$ over the time interval $[0, t]$, and the right panel illustrates the state of each cell.

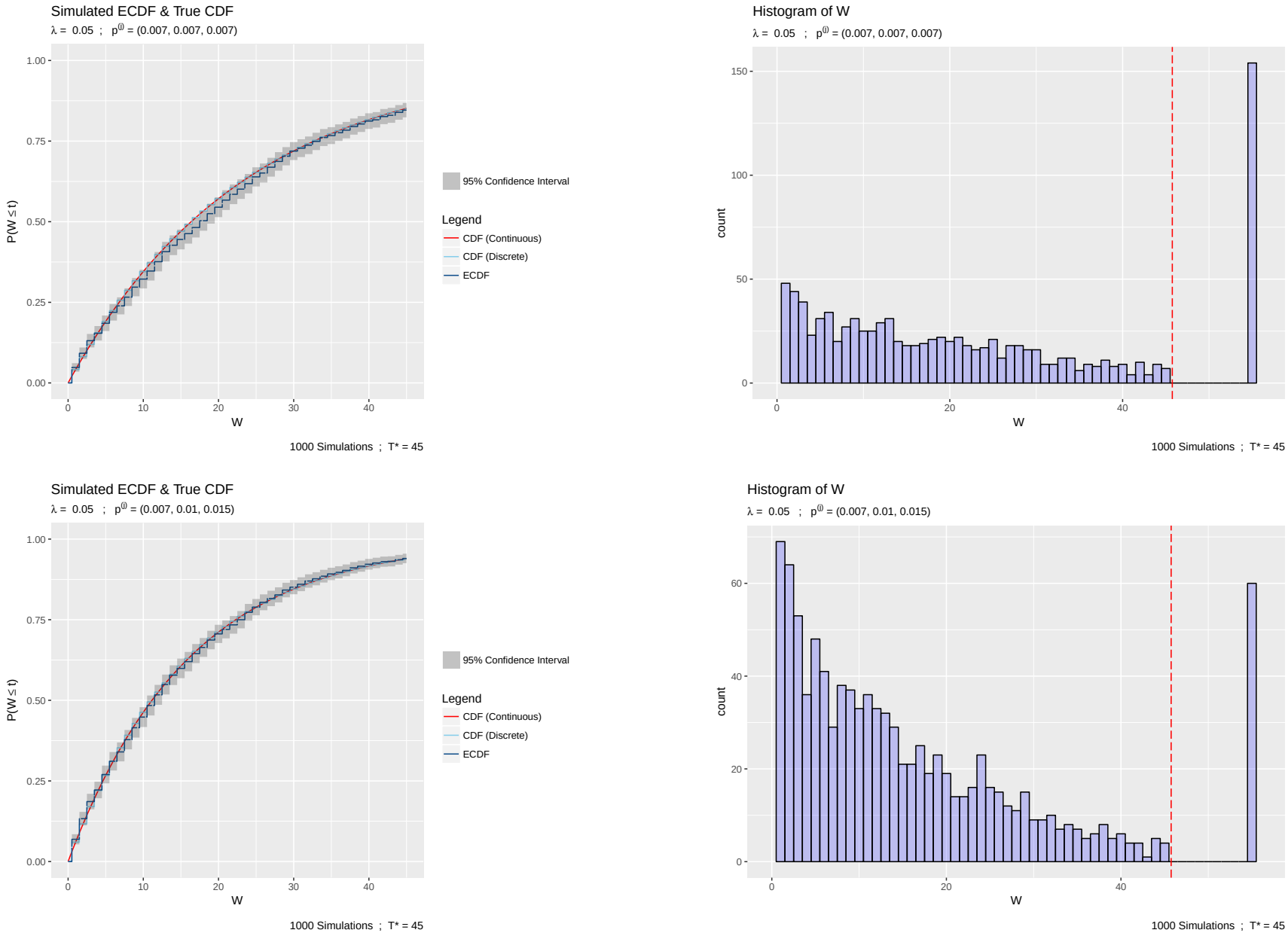

Figure A.4: Plots of the ECDF (left panel) and histogram (right panel) of W for the two simulation settings illustrated in Figures A.2 (top row) and A.3 (bottom row). The mass to the right of $W = T^*$ is $\hat{P}(W = \infty)$.

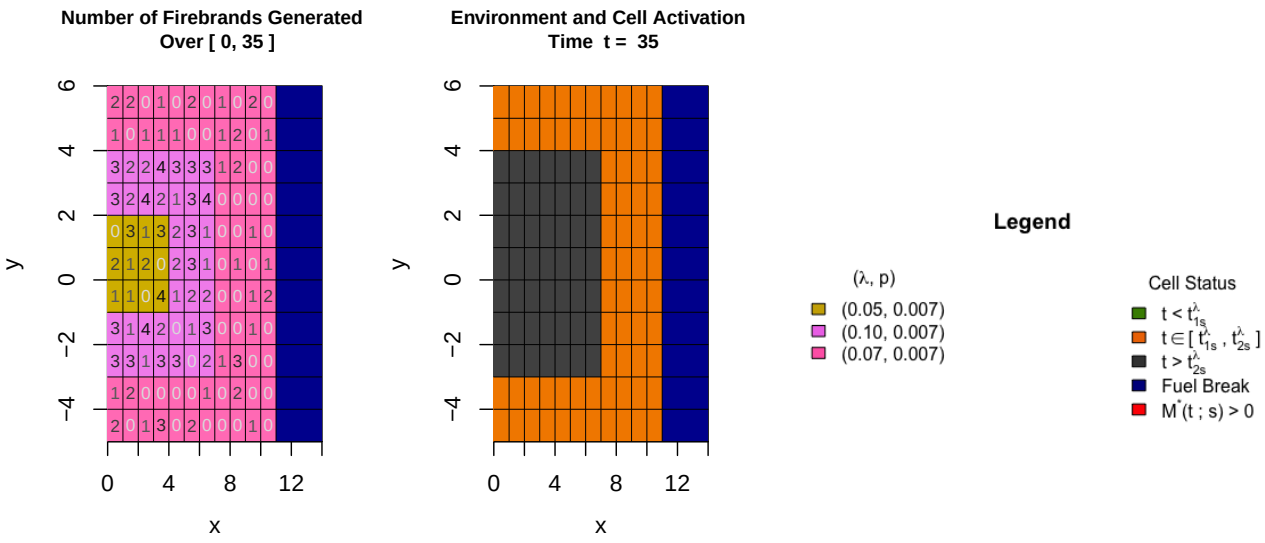

(a) All firebrands generated within cells $s \in \mathscr{S}$ have failed to result in a spot fire that crossed the fuel break.

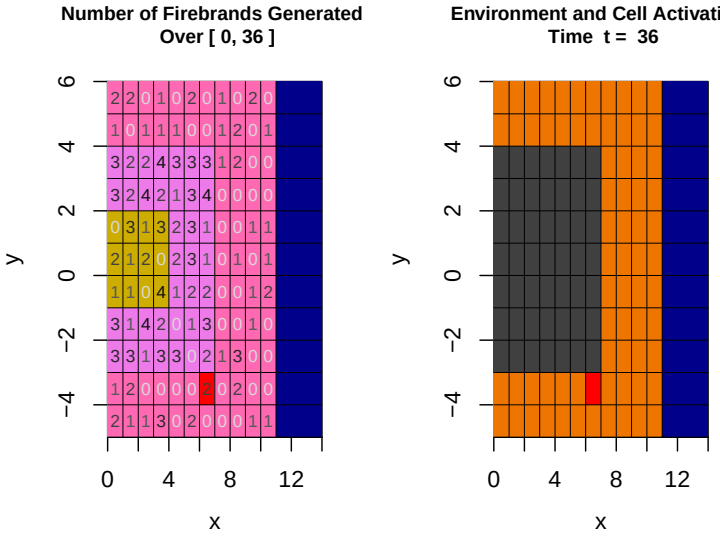

(b) A firebrand generated within cell $s = [6, 7] \times [-4, -3]$ results in a spot fire that crossed the fuel break.

Figure A.5: An illustration of the fire spotting procedure, where the left panel shows $N(t; s)$ for each $s \in \mathscr{S}$ over the time interval $[0, t]$, and the right panel illustrates the state of each cell.

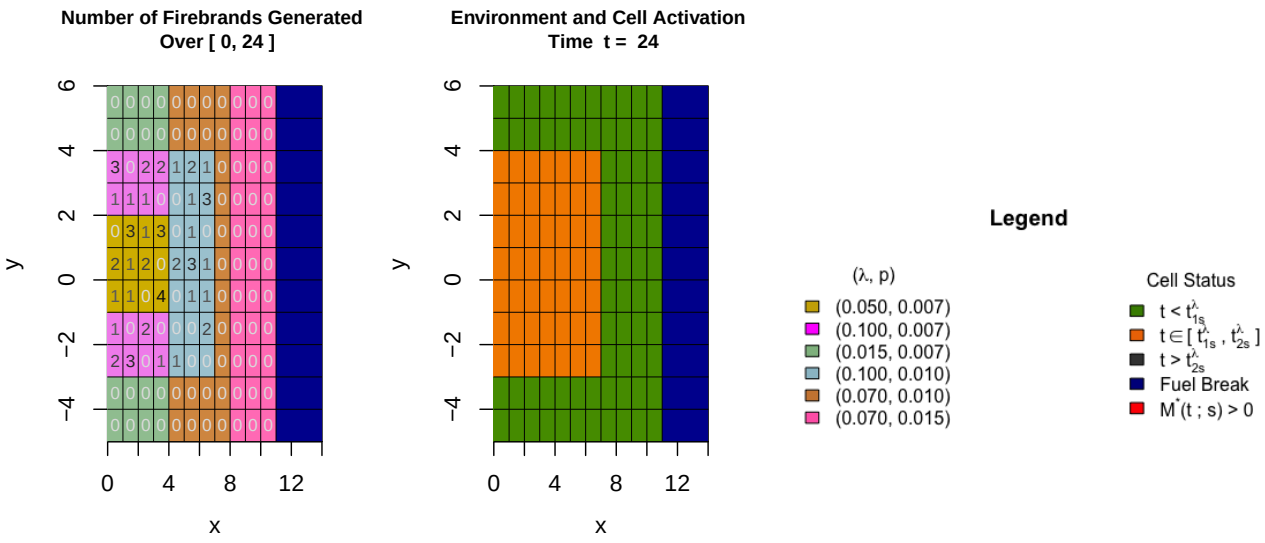

(a) All firebrands generated within cells $s \in \mathscr{S}$ have failed to result in a spot fire that crossed the fuel break.

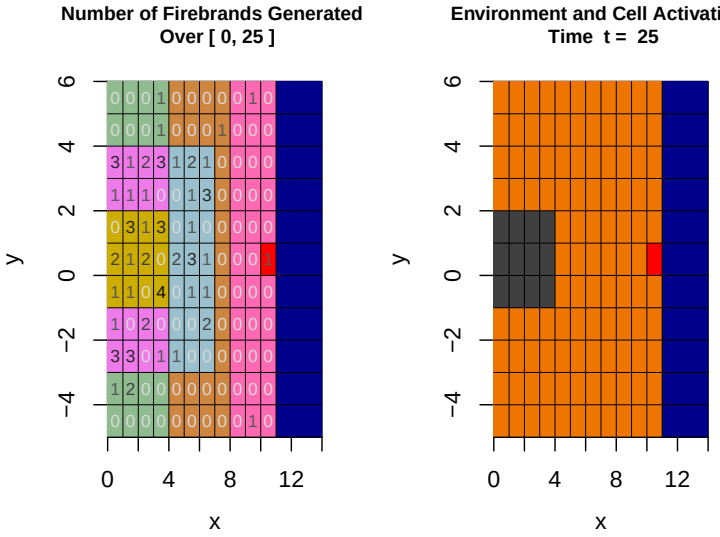

(b) A firebrand generated within cell $s = [10, 11] \times [0, 1]$ results in a spot fire that crossed the fuel break.

Figure A.6: An illustration of the fire spotting procedure, where the left panel shows $N(t; s)$ for each $s \in \mathscr{S}$ over the time interval $[0, t]$, and the right panel illustrates the state of each cell.

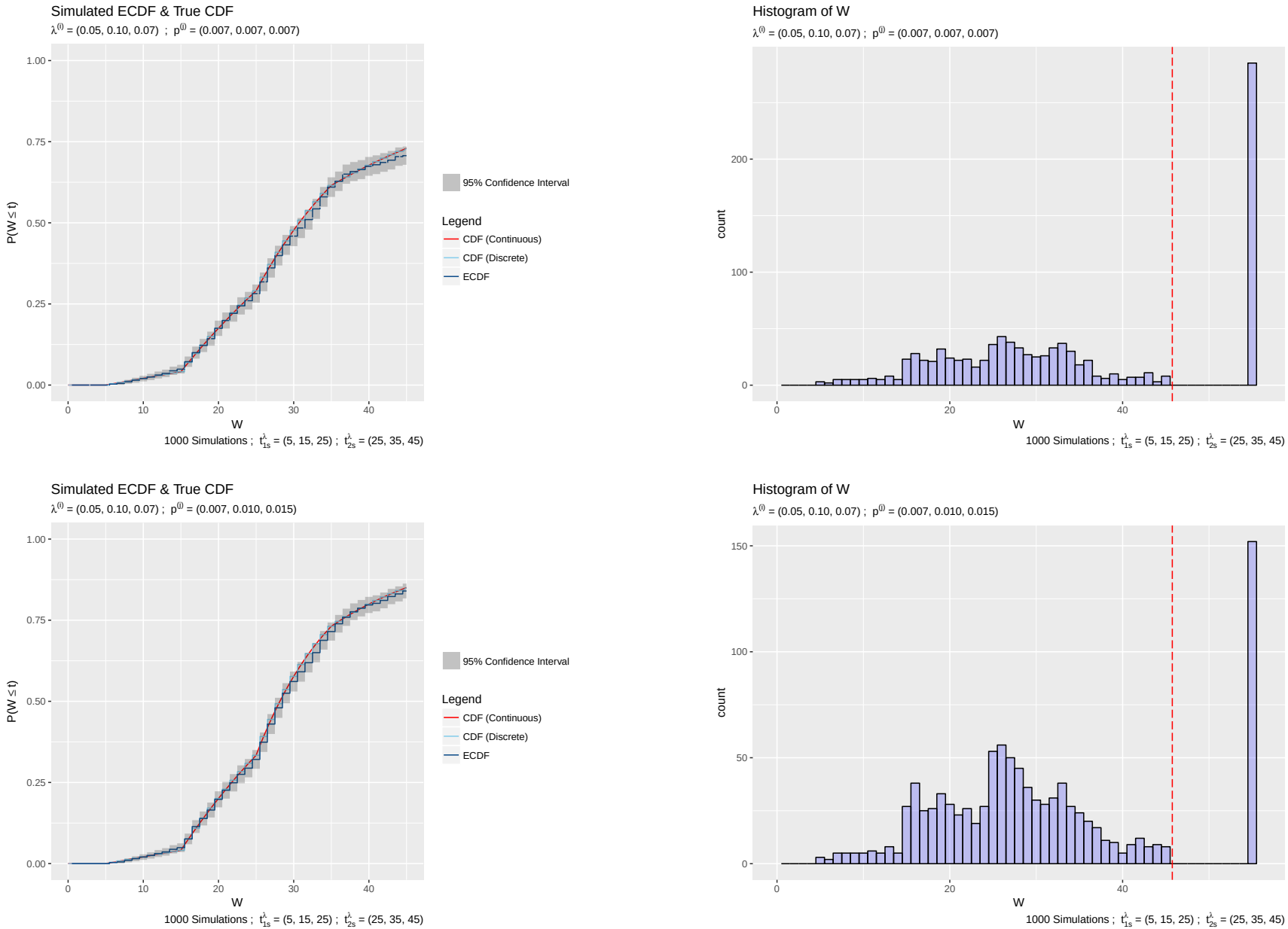

Figure A.7: Plots of the ECDF (left panel) and histogram (right panel) of W for the two simulation settings illustrated in Figures A.5 (top row) and A.6 (bottom row). The mass to the right of $W = T^*$ is $\hat{P}(W = \infty)$.

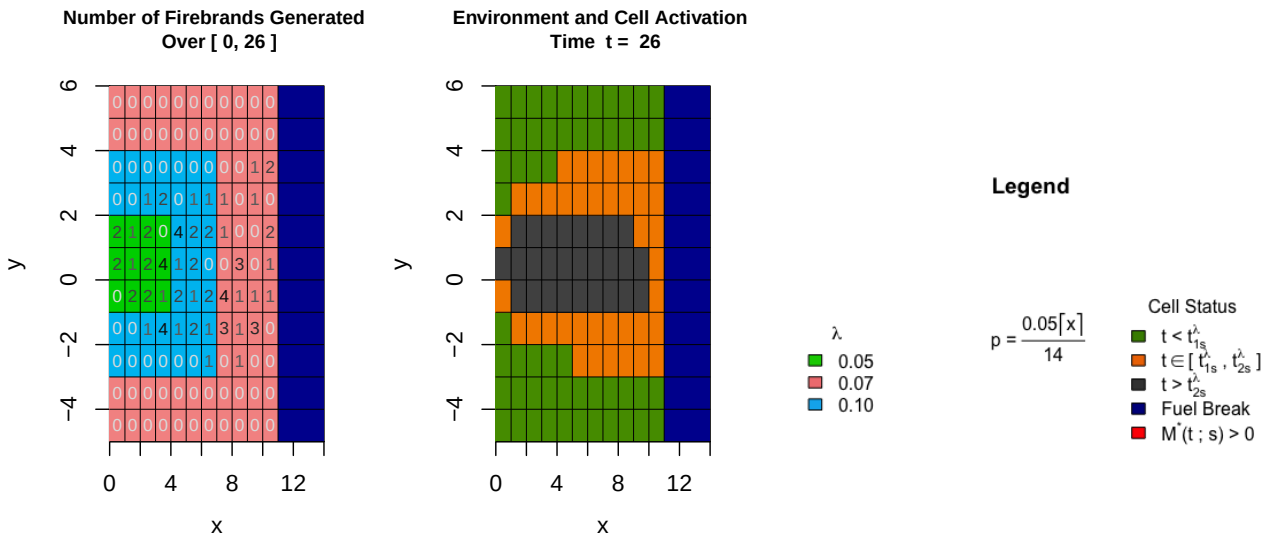

(a) All firebrands generated within cells $s \in \mathscr{S}$ have failed to result in a spot fire that crossed the fuel break.

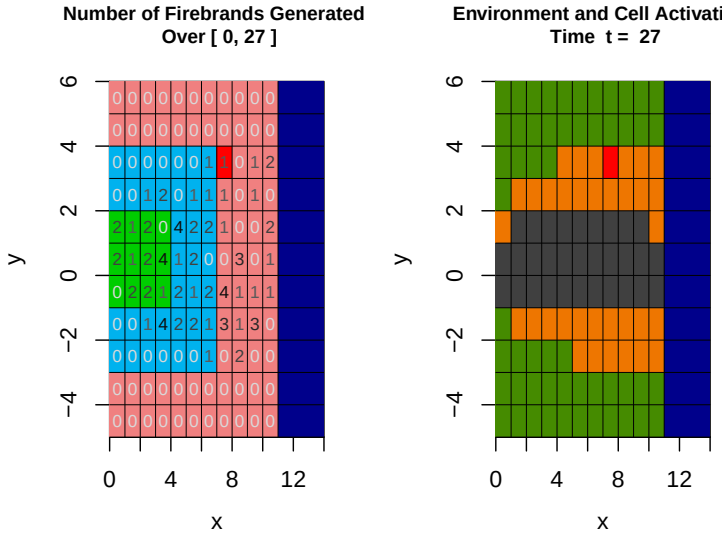

(b) A firebrand generated within cell $s = [7, 8] \times [3, 4]$ results in a spot fire that crossed the fuel break.

Figure A.8: An illustration of the fire spotting procedure, where the left panel shows $N(t; s)$ for each $s \in \mathscr{S}$ over the time interval $[0, t]$, and the right panel illustrates the state of each cell.

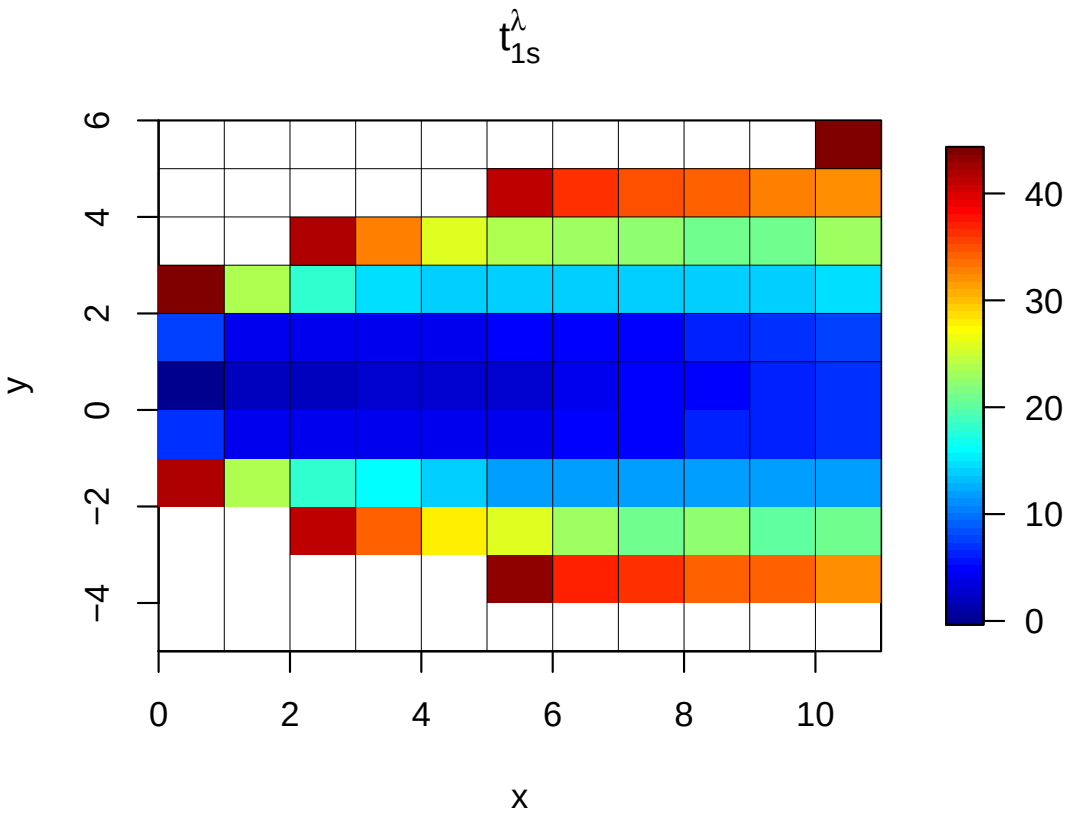

Figure A.9: A simulated realization of $\boldsymbol{t}_1^{\lambda}$ in accordance with the stochastic fire growth model presented in Chapter 3.2. Cells s coloured white indicate that $t_{1s}^{\lambda} > T^*$.

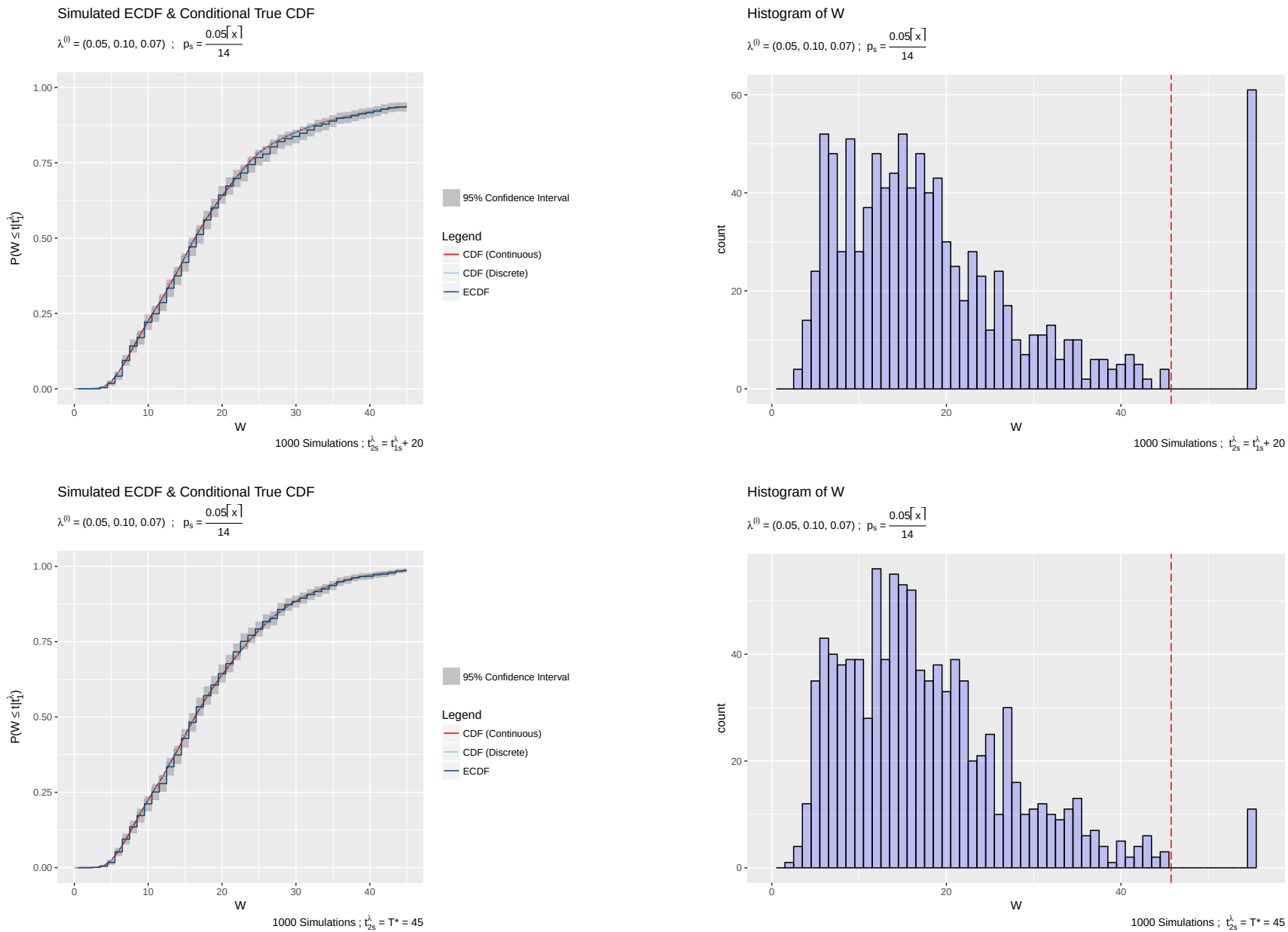

Figure A.10: Plots of the ECDF (left panel) and histogram (right panel) of W for the simulation setting illustrated in Figure A.8 (top row) and the case presented in Figure A.8 without burn-out (bottom row); conditional on $\boldsymbol{t}_1^{\lambda}$ illustrated in Figure A.9. The mass to the right of $W = T^*$ is $\hat{P}(W = \infty)$.

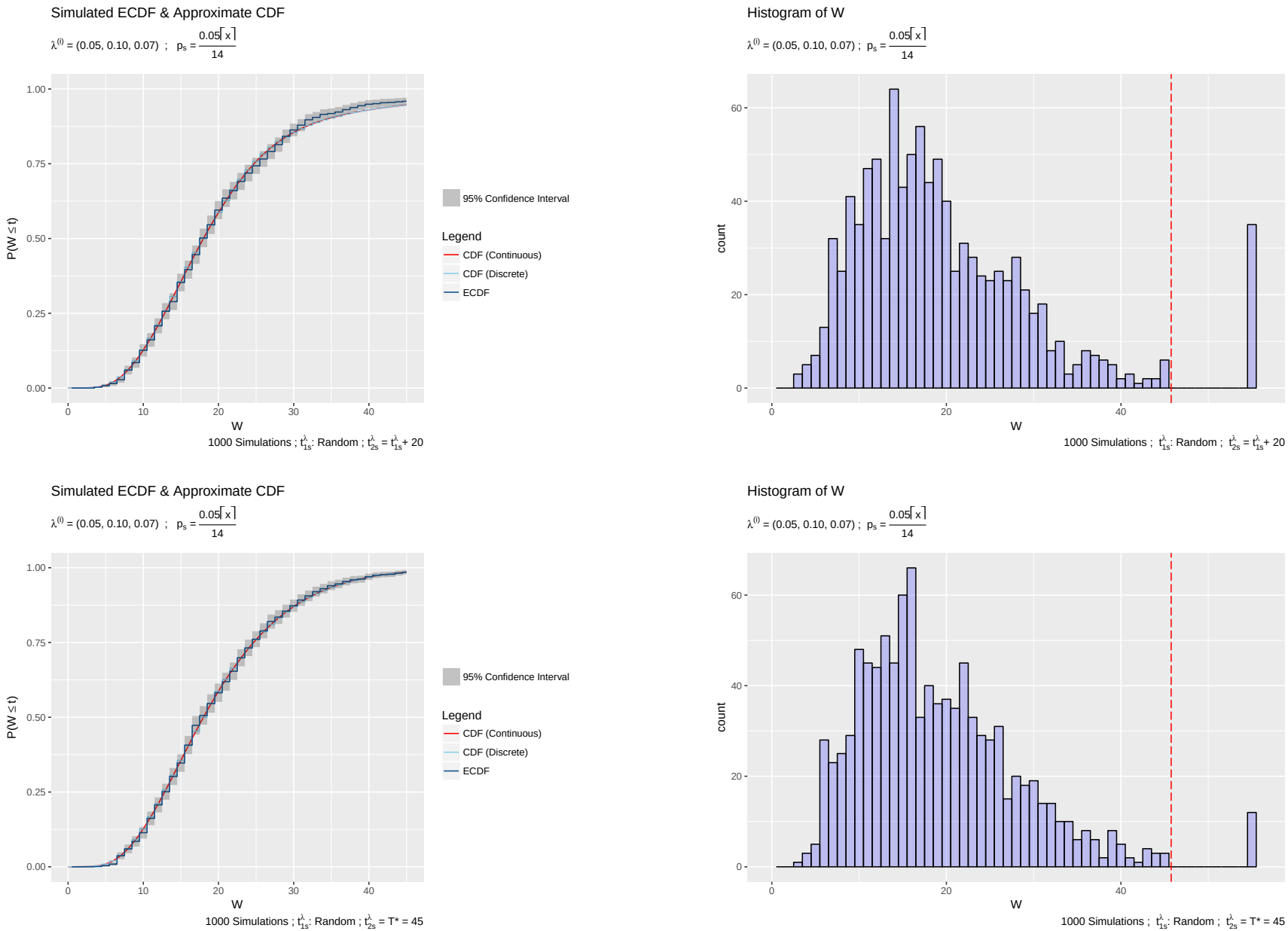

Figure A.11: Plots of the ECDF (left panel) and histogram (right panel) of W for the two cases presented in Figure A.10, except $\boldsymbol{t}_1^{\lambda}$ is random. The mass to the right of $W = T^*$ is $\hat{P}(W = \infty)$.

Appendix B

Plots for Additional Cases

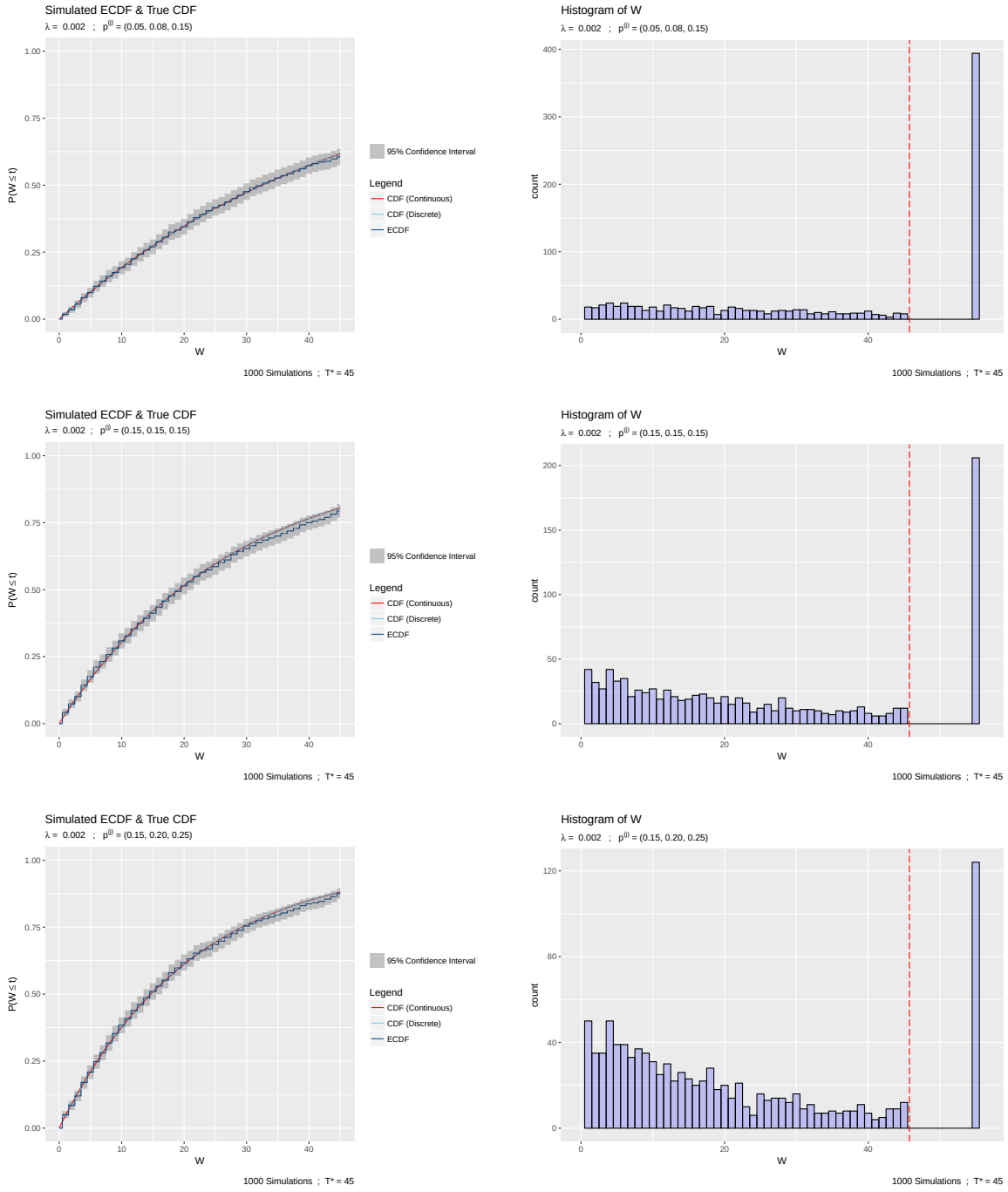

Figure B.1: Plots of the ECDF (left panel) and histogram (right panel) for additional cases presented in Table 3.1.

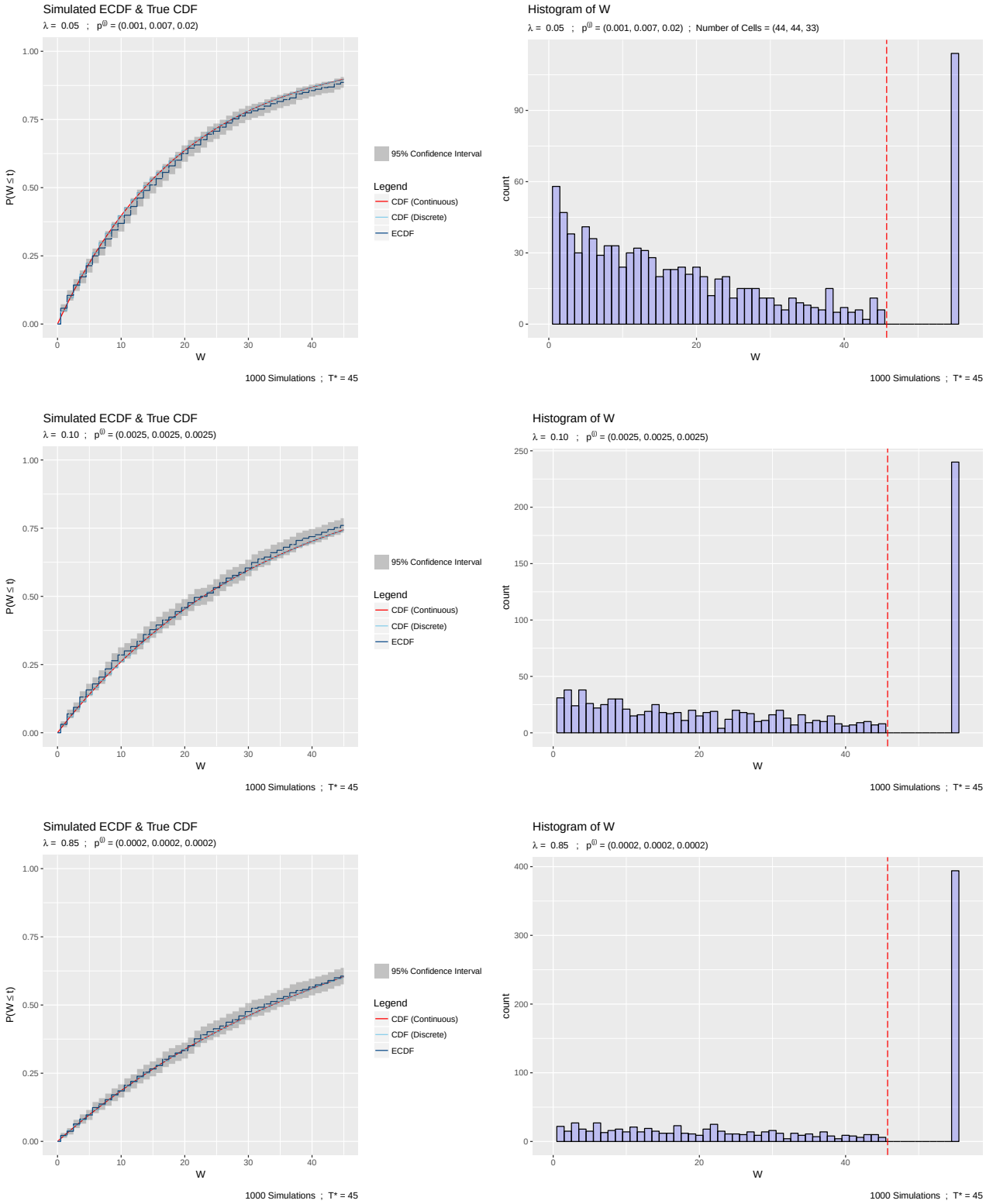

Figure B.2: Plots of the ECDF (left panel) and histogram (right panel) for additional cases presented in Table 3.1.

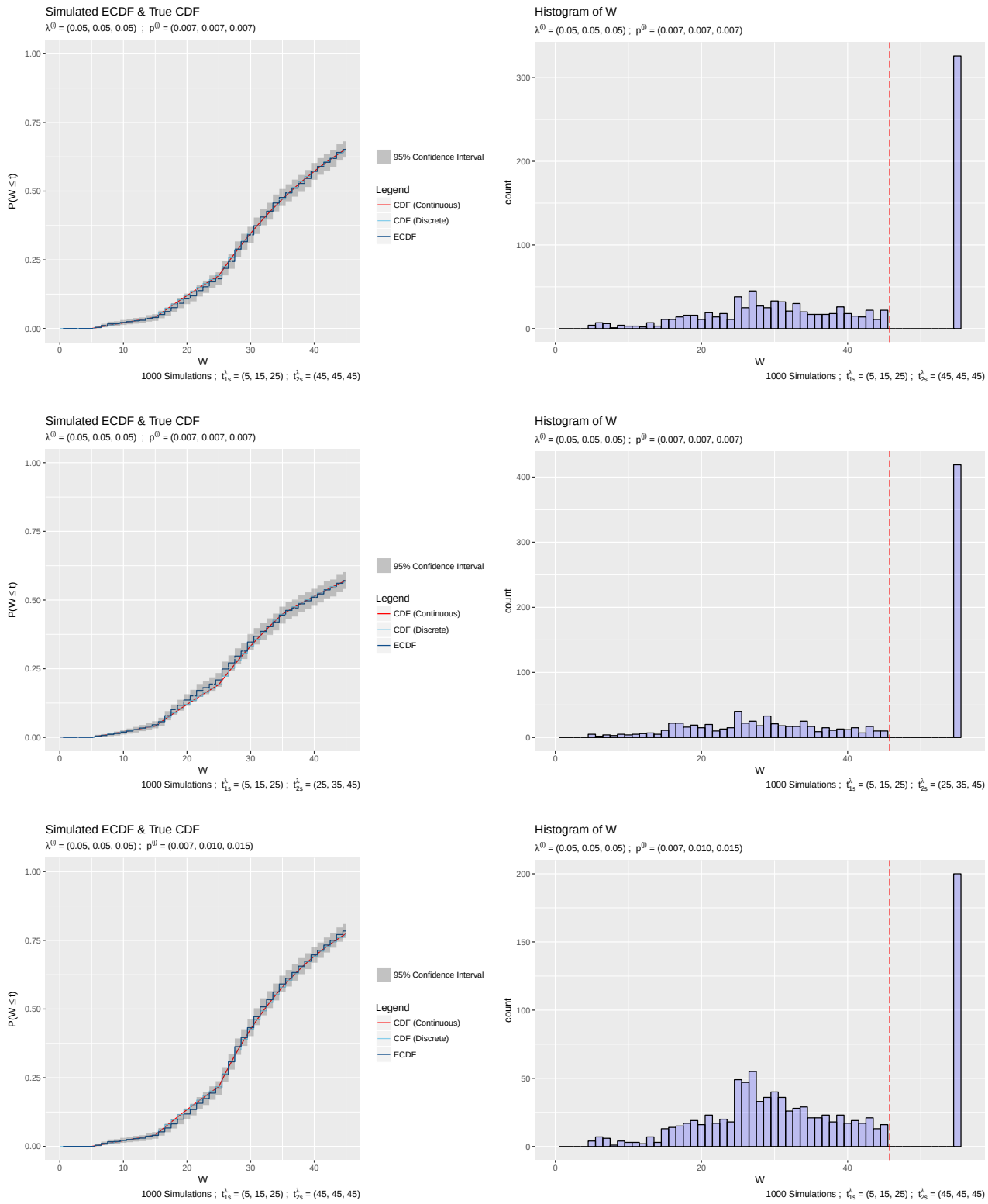

Figure B.3: Plots of the ECDF (left panel) and histogram (right panel) for additional cases presented in Table 3.2.

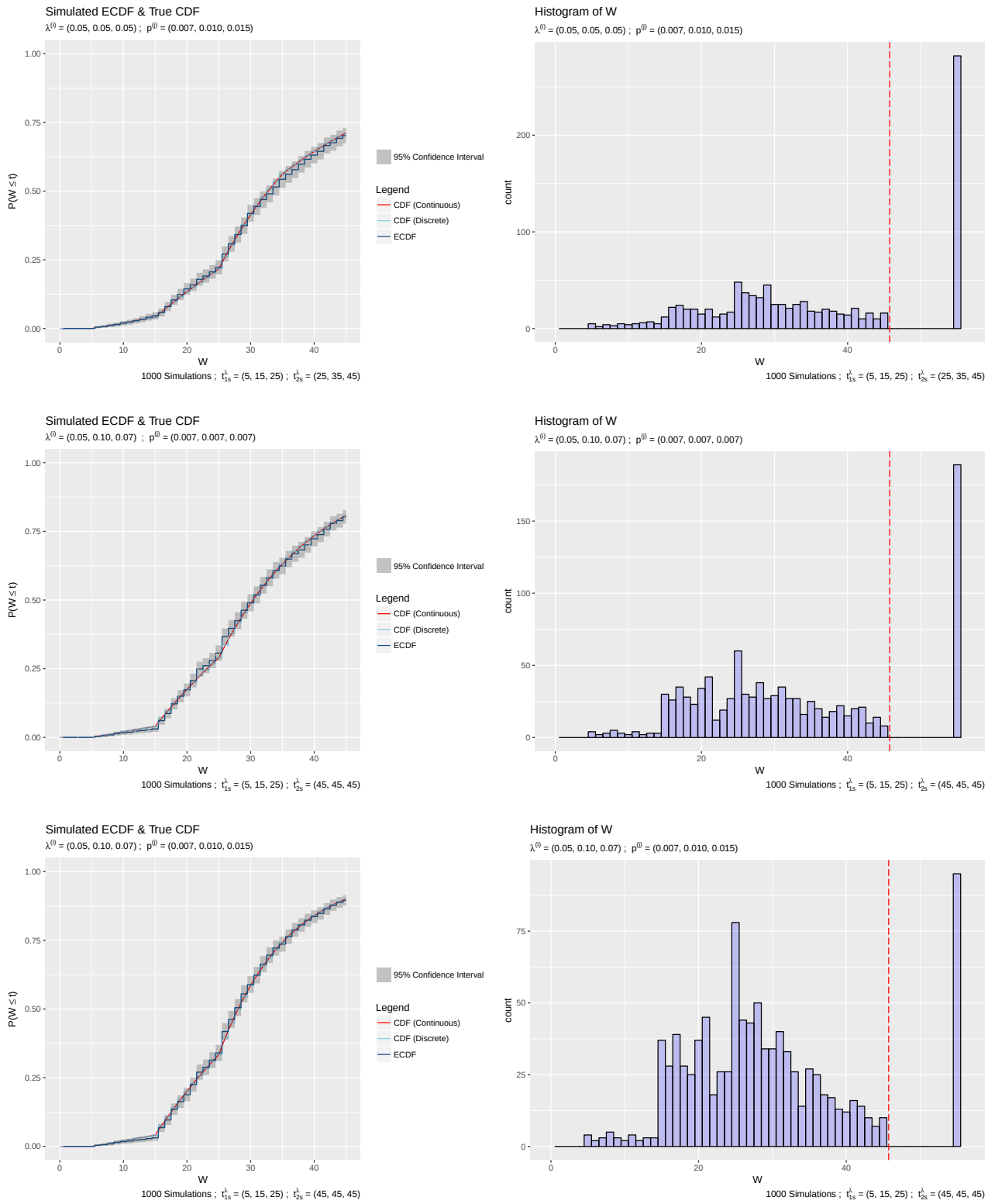

Figure B.4: Plots of the ECDF (left panel) and histogram (right panel) for additional cases presented in Table 3.2.

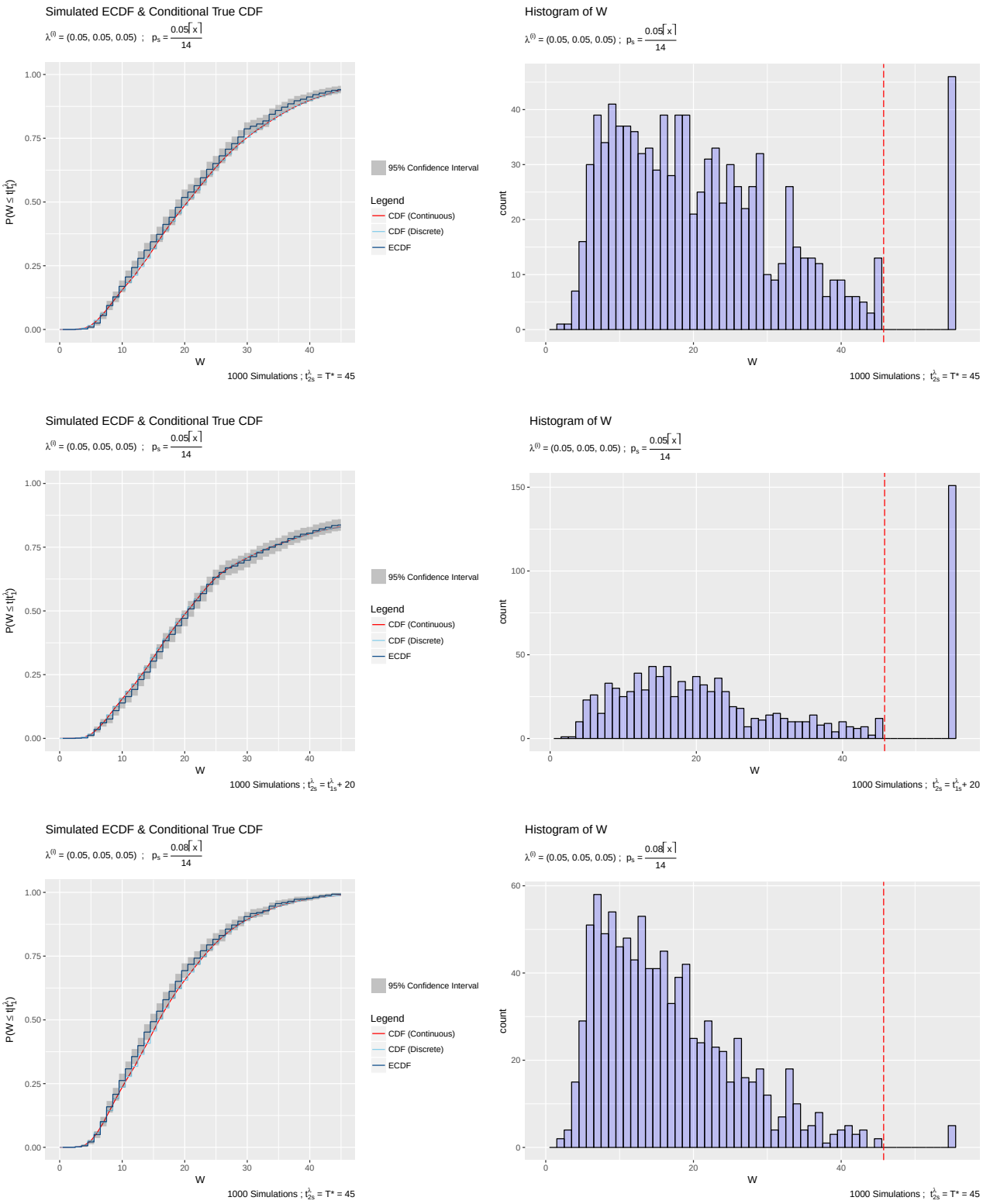

Figure B.5: Plots of the ECDF (left panel) and histogram (right panel) for additional cases presented in Table 3.3.

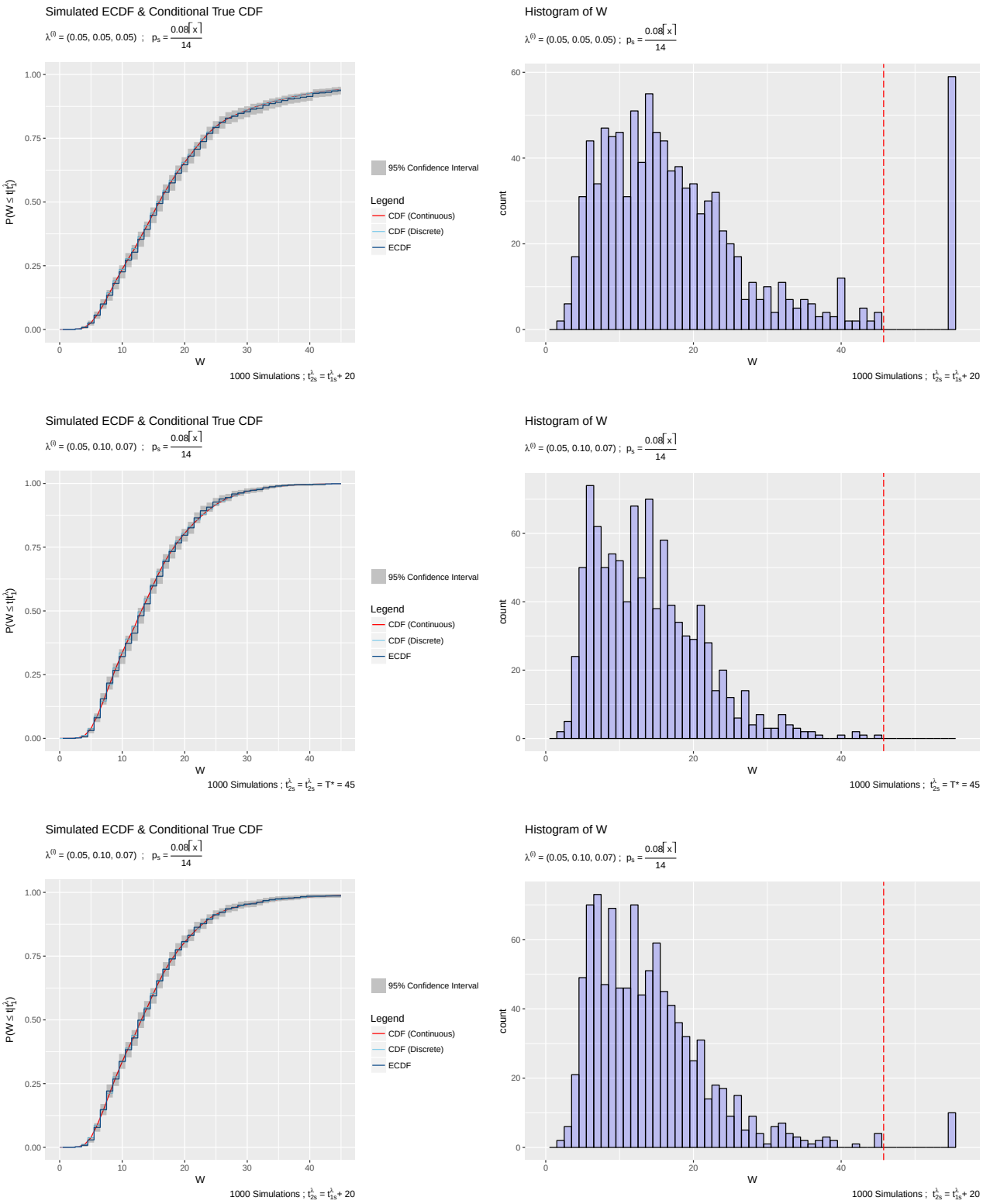

Figure B.6: Plots of the ECDF (left panel) and histogram (right panel) for additional cases presented in Table 3.3.

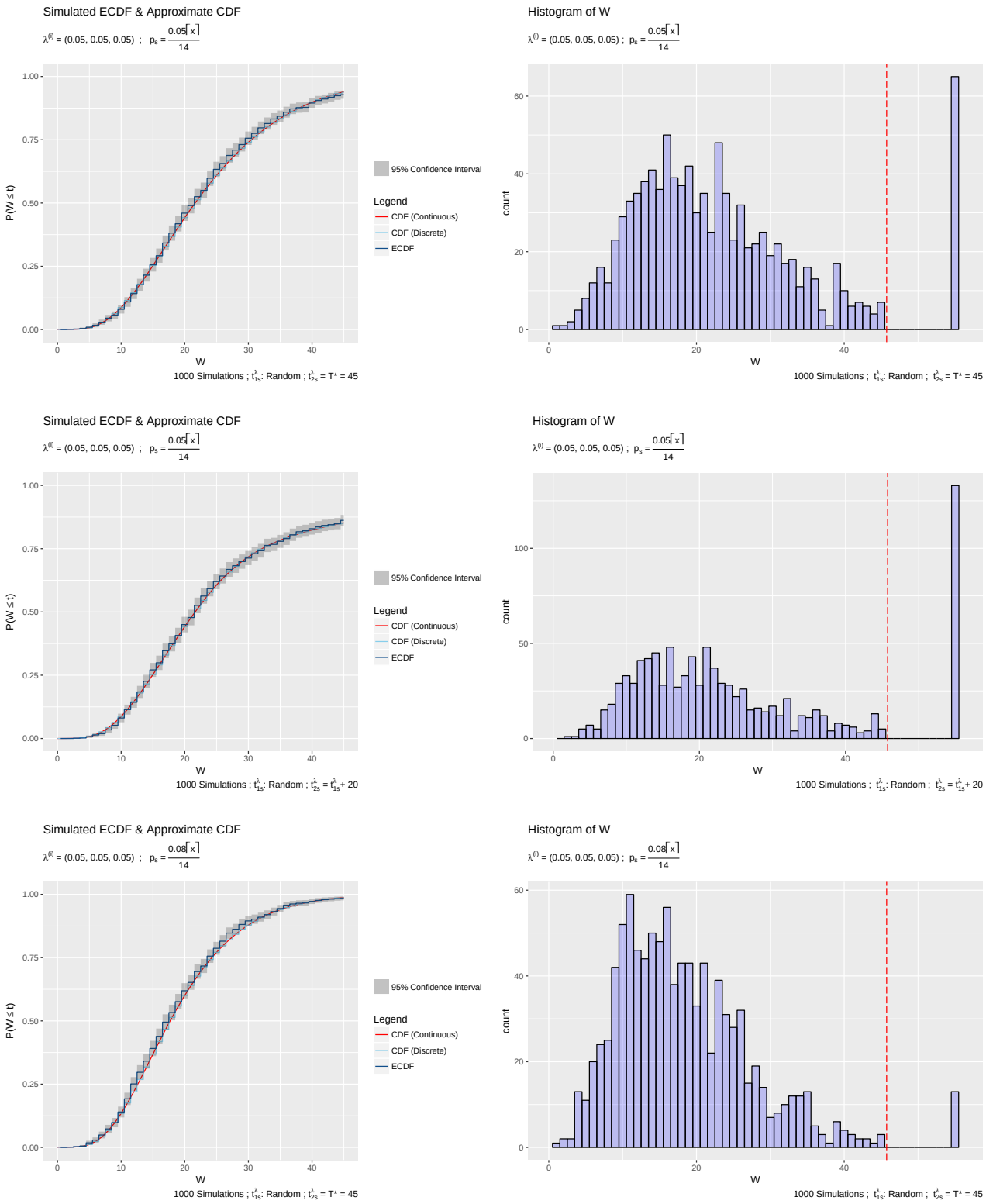

Figure B.7: Plots of the ECDF (left panel) and histogram (right panel) for additional cases presented in Table 3.4.

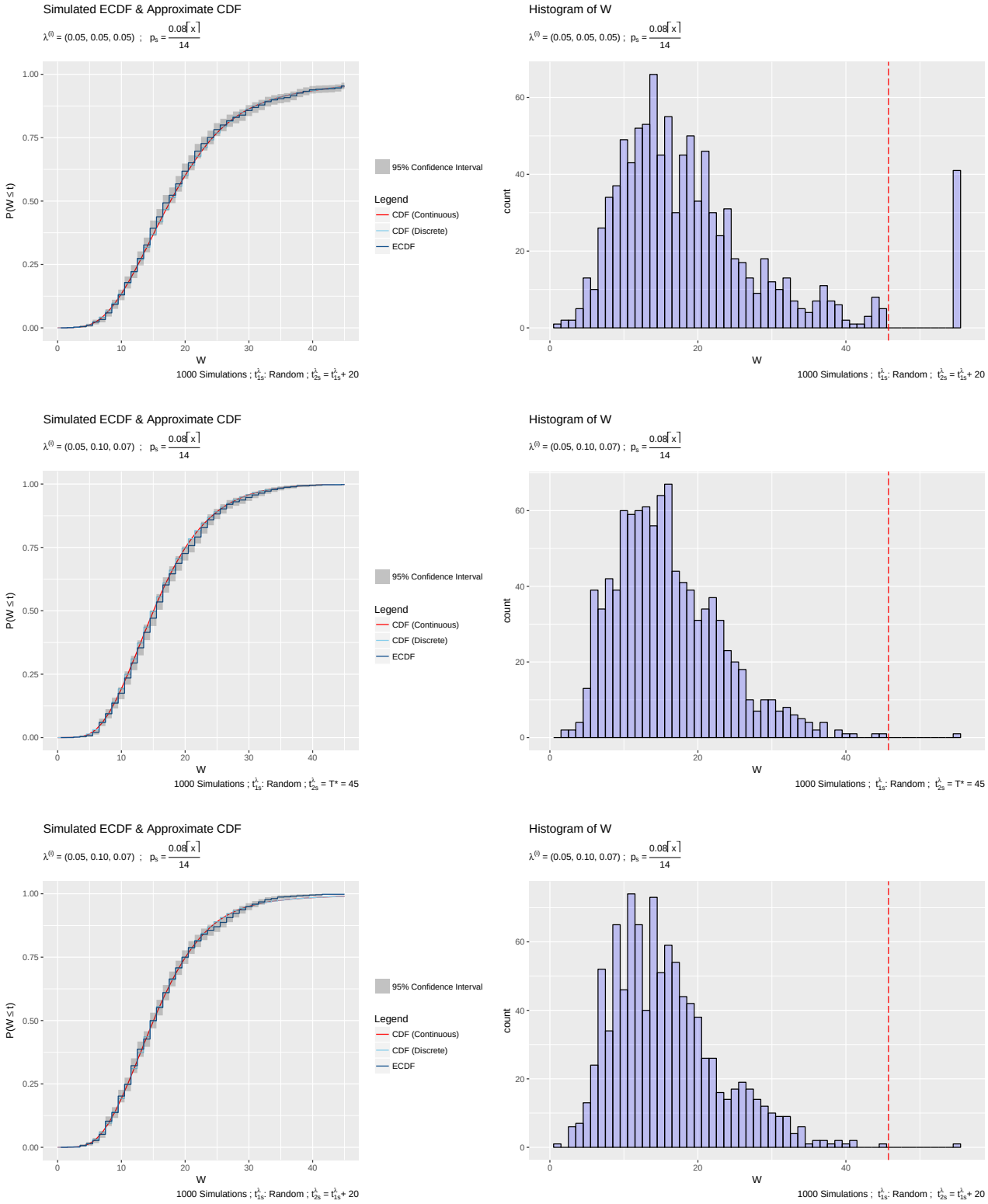

Figure B.8: Plots of the ECDF (left panel) and histogram (right panel) for additional cases presented in Table 3.4.